

Origami Biosystems: 3D Assembly Methods for Biomedical Applications

Vladimir A. Bolaños Quiñones, Hong Zhu, Alexander A. Solovev, Yongfeng Mei, and David H. Gracias*

Conventional assembly of biosystems has relied on bottom-up techniques, such as directed aggregation, or top-down techniques, such as layer-by-layer integration, using advanced lithographic and additive manufacturing processes. However, these methods often fail to mimic the complex three dimensional (3D) microstructure of naturally occurring biomachinery, cells, and organisms regarding assembly throughput, precision, material heterogeneity, and resolution. Pop-up, buckling, and self-folding methods, reminiscent of paper origami, allow the high-throughput assembly of static or reconfigurable biosystems of relevance to biosensors, biomicrofluidics, cell and tissue engineering, drug delivery, and minimally invasive surgery. The universal principle in these assembly methods is the engineering of intrinsic or extrinsic forces to cause local or global shape changes via bending, curving, or folding resulting in the final 3D structure. The forces can result from stresses that are engineered either during or applied externally after synthesis or fabrication. The methods facilitate the high-throughput assembly of biosystems in simultaneously micro or nanopatterned and layered geometries that can be challenging if not impossible to assemble by alternate methods. The authors classify methods based on length scale and biologically relevant applications; examples of significant advances and future challenges are highlighted.

1. Introduction

Biological structures ranging in size from molecular machines such as the ribosome to organelles, cells, multicellular organisms, organs, and the human body are exquisitely structured with hierarchical precision and significant material heterogeneity in all three dimensions.^[1,2] In order to mimic, sense, and record signals, or to interface synthetic systems with biological


ones, there is a need to create integrated biosystems that are similarly structured from nano to macrolength scales.^[3–8] Like naturally occurring biological systems, it is also important that assembly and integration be achieved in a high-throughput and parallel manner. Integration in this context implies the incorporation of different materials and functionalities with precise spatiotemporal characteristics. Concerning material composition, biology combines soft materials (e.g., protein gels such as collagen), hard materials (e.g., inorganics such as hydroxyapatite), cells, and fluids of varying viscosity (e.g., interstitial fluid and blood plasma). In terms of functionality, biology is replete with complex 3D interconnected systems for fluid flow, transmission of electrical signals, growth, regeneration, and maintenance of homeostasis, all of which require 3D hierarchical synthesis, patterning, and assembly.^[9]

Many methods can be utilized for synthesis, patterning, and assembly with varying advantages and disadvantages. They are broadly classified into bottom-up or top-down approaches. Bottom-up approaches often rely on directed synthesis or self-organization by aggregation.^[10–14] These methods can be utilized to create hierarchical assemblies with a wide range of materials including organics, inorganics, and hybrids via a variety of forces including covalent, ionic or hydrogen bonds and van der Waals, hydrophobic, electrostatic or magnetic interactions.^[15,16] As we discuss in this review, aggregation can be augmented by strain engineering to enable the assembly of more complex structures composed of bent or folded molecules and their aggregates.

Popular top-down methods include conventional layer-by-layer photo, electron beam, or replica patterning using additive or subtractive thin-film deposition techniques.^[17–21] These techniques can be highly parallel and precise but are inherently 2D; they typically involve the serial deposition or removal of a material with a prescribed pattern transferred using computer-aided design generated optical masks, programmed electron beam raster controls, or relief molds. Using these techniques, it can be relatively easy to create inherently planar structures but challenging to create entirely curvilinear geometries.

Dr. V. A. Bolaños Quiñones, H. Zhu, Prof. A. A. Solovev, Prof. Y. Mei
Department of Materials Science
State Key Laboratory of ASIC and Systems
Fudan University
Shanghai 200433, P. R. China

Prof. D. H. Gracias
Department of Chemical and Biomolecular Engineering
Johns Hopkins University
3400 N Charles Street, 221 Maryland Hall, Baltimore, MD 21218, USA
E-mail: dgracias@jhu.edu

 The ORCID identification number(s) for the author(s) of this article can be found under <https://doi.org/10.1002/adbi.201800230>.

DOI: 10.1002/adbi.201800230

The recent revolution of additive manufacturing has opened up a range of techniques for nozzle-based deposition or stereolithography. These methods enable customizable patterning with low material costs but with limited material classes, spatial resolution, and throughput.^[22,23] Additive manufacturing methods have been utilized to print a range of biological materials including gels and cells, but the integration of dissimilar classes of materials such as metals, with polymers, and complex components such as fluidic or pneumatic microchannels as would be required for robots or biosensors can be challenging.^[24,25] Likewise, 3D nanoscale patterning techniques such as focused ion beam milling have limited fabrication throughput and capabilities for complex integration and assembly.^[26]

One emerging class of methods achieves this integration of biosystems by changing the shape of previously synthesized molecules, films, sheets, or 3D printed structures by bending, curving, and folding. Reminiscent of the ancient art of origami, these methods utilize either manual or self-folding to create integrated structures with 3D form and function. There are many review articles on molecular and thin-film assembly approaches based on folding; the reader is directed to several recent reviews on molecular folding^[27–34] and to reviews on static and reconfigurable curving and folding of thin films.^[35–56] Here, we focus on unifying assembly methods based on manipulation of shape by bending, curving, and folding and on uncovering underlying principles across length scales from molecules to the macroscale, with a focus on integrated systems of relevance to biology and medicine.

We note that there are several important features of this approach. First, the approach of shaping structures by strain engineering is intellectually stimulating and inherently bioinspired. Many biological systems are assembled when intrinsic or extrinsic forces shape their final structure by bending, curving, and folding. Also, assembly approaches are observed at a variety of length scales ranging from molecular to macroscale. For example, proteins assemble their exquisite 3D structures by folding. In this case, 3D assembly is driven by a balance of intra and intermolecular forces (e.g., electrostatic, hydrogen bonding, and hydrophobic effect) that bend and fold the molecule into its final secondary and tertiary structures.^[57] In the cellular world, one of the widely observed assembly processes in multicellular embryonic morphogenesis is the bending, invagination, exvagination, and folding of the epithelium.^[58–60] In these processes, forces derived from differential swelling of either apical or basal portions of groups of epithelial cell sheets cause spontaneous curving and folding of tissues.^[61,62] At a larger length scale, and as an example of a naturally occurring dynamic process, the complex folding and unfolding mechanisms of the wings of ladybird beetles are associated with complex origami crease patterns.^[63,64] Throughout the review, we provide examples of strain-engineered systems associated with bending, curving, and folding in biology and nature.

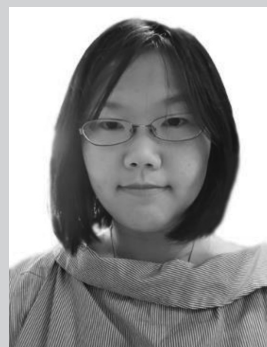
Second, forces required to bend, curve, and fold structures can be applied during or after aggregative, planar, layered, or additive patterning. This is evident in the naturally observed spontaneous curving of phospholipid bilayers, where molecular rafts aggregate with their nonpolar groups oriented away



Vladimir A. Bolaños Quiñones

received his Ph.D. in physics from the Chemnitz University of Technology for his research work at the Leibniz Institute for Solid State and Materials Research, Dresden. Currently, he is a postdoctoral research fellow at the Department of Materials Science at Fudan University. His research interests include optical

microcavities and their applications as analytical sensors, microrobots, and optofluidics platforms.



Hong Zhu is a Ph.D. stu-

dent at the Department of Materials Science at Fudan University. She received her B.S. in the College of Nanoscience and Technology from Suzhou University in 2017. Her research focuses on the development of hydrogels and their applications as micromotors and actuators.



Alexander A. Solovov received

his Ph.D. from the Institute for Integrative Nanosciences, Leibniz Institute for Solid State and Materials Research Dresden. He was a postdoctoral fellow with Geoffrey Ozin at the University of Toronto and visiting scholar with David Weitz at Harvard. Currently, he is a young “1000 talent” professor at the Department of

Materials Science, Fudan University, Shanghai, P. R. China. His research group interests include new properties of 3D nanomembranes, microfluidics, clean energy, autonomous, and collective behavior of nano/micromotors.

from the aqueous medium and curve up to balance aggregation, bending, and surface energies.^[14,65,66] Assembly by bending, curving, and folding can be applied to thin films that have been patterned by photo, electron, ion beam, or imprint lithography approaches.^[49,51,67] These lithographic patterning approaches are well established for the microchip and microfluidics industry, and they can enable highly resolved patterns down to the nanoscale. For example, capillary forces have been utilized to fold up polyhedra from precursor films that were patterned by e-beam lithography with well-resolved features as small as 15 nm.^[68] More recently, shape change has also been utilized with nanoimprint patterned thin films, which suggests

that high-throughput nanomanufacturing of 3D structures may be possible.^[69] Heterogeneous patterning can also endow optical or electronic functionality into the curved or folded structures. These features such as high-throughput assembly of layered, functional, and nanostructured devices are advantages over alternate 3D fabrication techniques such as 3D printing, for example, which has limited 3D spatial resolution and is a serial approach. Recently, the so-called 4D printing and 4D biofabrication methods have been reported; these involve the programmed and dynamical shape change of 3D printed structures.^[70–73] The 4 in “4D” refers to the fourth dimension reflecting a temporal change of the structure after 3D printing.

Third, origami-inspired assembly methods can be applied to previously patterned and layered thin films to form tubular, polyhedral, or complex 3D structures wherein fluidic or gaseous channels are integrated into the side walls.^[56,74] Since layering, patterning, and curvature are all present simultaneously in many tissues such as the bladder, intestine, cartilage, blood vessels, or mammary ducts,^[75,76] origami assembly approaches that permit the curving and folding of previously layered and patterned thin films are highly relevant to tissue engineering.

Finally, strain-engineered methods also enable the creation of integrated biosystems with compact form factors that permit small overall sizes of relevance to smart dust sensors and untethered miniature robots. This point is especially relevant to devices composed of 2D layered materials that offer unique physical and chemical properties but occupy large space due to their planar geometry.^[77,78]

We now describe these origami biosystems that are broadly defined as integrated and functional devices, structures, or platforms of relevance to biology and medicine that have been created by local or global strain manipulation of precursors resulting in bending, curving, or folding. We can classify origami biosystems based on relevance to biomolecular assembly, biosensors, biomicrofluidics, cell/tissue engineering, drug delivery, and biorobotics (Figure 1). These classes broadly reflect the breadth of activity in origami biosystems and are described in more detail below. In each case, bending, curving, and folding of molecules, thin films, or 3D shapes enables their structure and function.

2. Biomolecular Assembly

The 3D assembly process and resulting structure of complex biomolecules exemplify the importance of curvature and folding approaches seen in biology. The machinery in organisms involves proteins and more complex biomolecules such as the ribosome that often function only in specific 3D folded states.^[79] Many diseases such as cystic fibrosis and many neurodegenerative diseases are thought to be caused by misfolded proteins.^[80] Since the total number of conformations that biomolecules, such as proteins, can adopt is enormous, nature has evolved many advanced design concepts for efficient folding. In the crowded cellular space where the cytosolic protein concentration can be as high as 400 g L^{-1} , the balance between aggregation and folding is indeed very delicate, and can be the balance between life and death.^[81] Consequently, natural protein folding involves the exquisite design of funnel-shaped

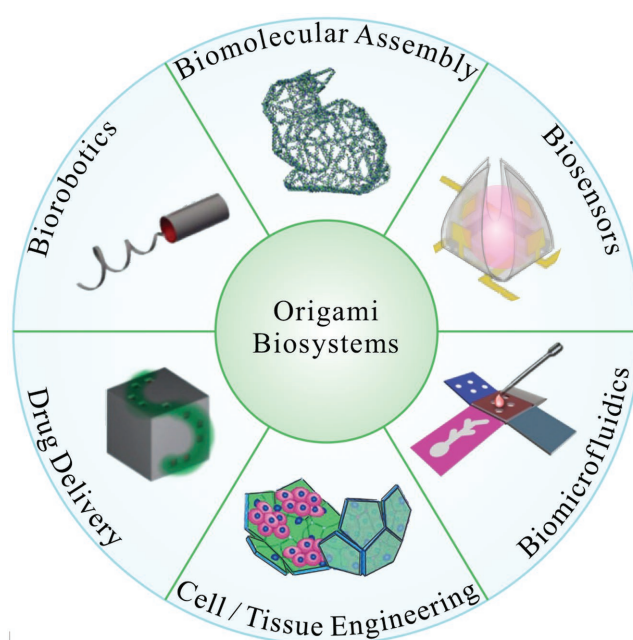


Figure 1. Schematic classification of origami biosystems. Biomolecular assembly. Adapted with permission.^[300] Copyright 2015, Springer Nature. Biosensors. Adapted under the terms and conditions of the Creative Commons Attribution license 4.0.^[115] Copyright 2018, the authors, published by Wiley-VCH. Biomicrofluidics. Adapted with permission.^[172] Copyright 2012, The Royal Society of Chemistry. Cell and tissue engineering. Adapted with permission.^[235] Copyright 2018, Springer Nature. Drug delivery. Adapted with permission.^[252] Copyright 2011, Wiley-VCH. Biorobotics. Adapted with permission.^[284] Copyright 2016, Springer Nature.

potential energy surfaces that minimize folding errors and the use of molecular chaperones that stabilize selected conformations and aid protein folding.^[82]

Naturally occurring biomolecular folding is not just restricted to proteins but also observed in other naturally occurring molecular systems such as DNA, RNA, or hybrid polynucleotide–protein structures. A classic example is chromatin that is an assembly where DNA wraps around histone proteins to form nucleosomes and then larger curved and folded geometries.^[83] The small final form and shape of chromatin illustrates the usefulness of curving and folding approaches in packaging structures in a small space while at the same time providing accessibility to interactions with the external environment.^[84]

Due to the observed exquisite nature of natural biomolecular folding, a long-standing dream in macromolecular chemistry has been to create synthetic molecules that would mimic naturally folded biomolecules and fold up into specific conformations.

2.1. Foldamers

The term foldamer broadly refers to oligomers or polymers that fold into compact or conformationally ordered shapes with primary and secondary structure.^[27,28] A variety of synthetic approaches have been utilized to manipulate the folding

of molecular chains. For example, the manipulation of local rigidity and stacking in synthesized molecular chains composed of heterocycles with extended hydrazone and pyrimidine sequences has allowed programming of molecules that fold into helical shapes.^[85] Peptidomimetic foldamers consist of modified amino acids that stabilize secondary structures and fix specific portions of the molecule while mini-proteins are short polypeptide chains, typically <40 amino acids in length that can fold into 3D structures.^[32] In order to design secondary structures, β -peptide homopolymers can be utilized to create sheets while α -peptides can be utilized to create sinusoidal or helical shapes. Due to the small size of mini-proteins, there are fewer noncovalent (e.g., hydrophobic) interactions as compared to proteins, and so they must often be stabilized by covalent interactions and metal ion stabilization. Elsewhere, vinylous amino acids, oligosulfonamides, aedamers, and a variety of oligomers have been utilized to fold molecules into 3D structures based on donor–acceptor interactions, H-bonds, polar, and hydrophobic interactions.^[86–88] Significant challenges exist in extending the complexity of synthetic foldamers

beyond their secondary structure to more complex tertiary structures and fine tuning the interactions to realize funnel-shaped potential energy landscapes to minimize erroneous side products.

2.2. Synthetic Folding DNA

As a consequence of the predictable hydrogen base pair binding of nucleotides, complementary strands of DNA or RNA can be designed to fold up into complex 3D structures via Watson–Crick base pairing.^[33,89] As compared to foldamers that interact by a variety of forces, DNA folding can be programmed and consequently is amenable to design; i.e., the inverse problem of designing precursor molecular strands that can fold into a predictable final shape is more tractable. Synthetic folding of single-stranded DNA structures can broadly be classified into three methods (Figure 2). They include folding with all short strands, folding with a long and several short strands, and folding of a single long strand.^[30,90–94] Each method has

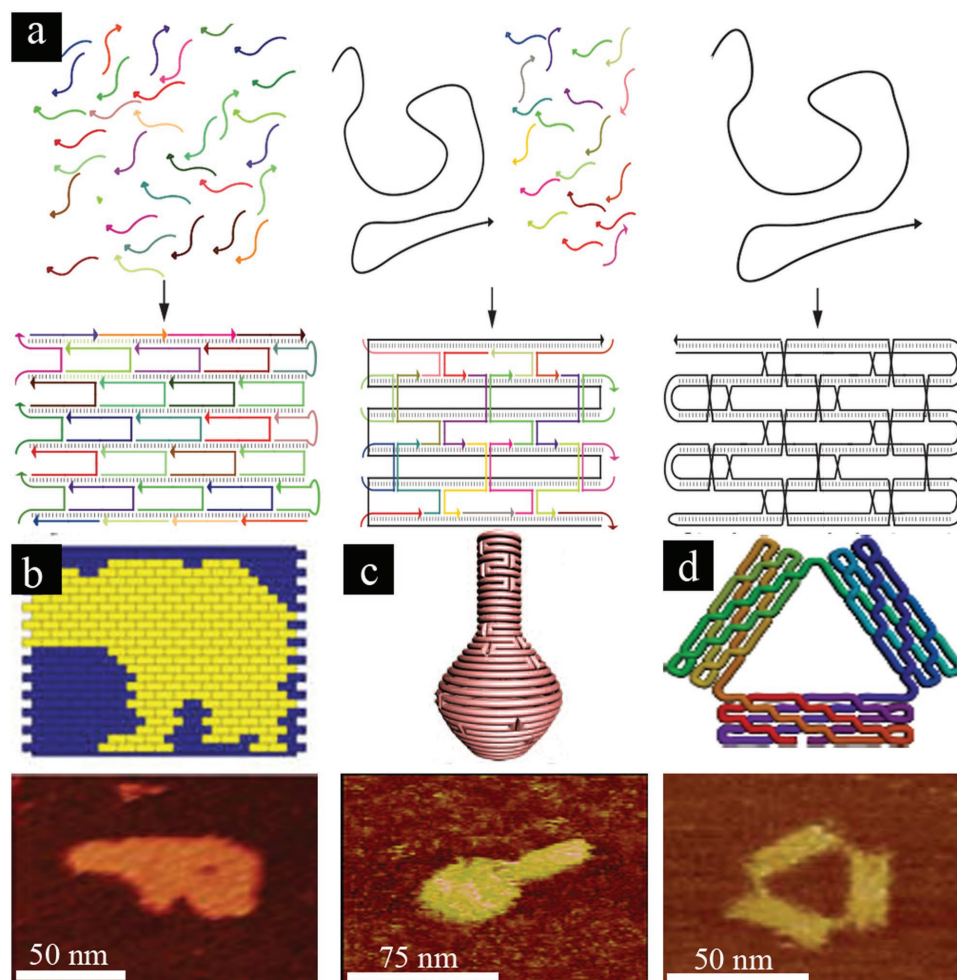


Figure 2. Major classes of DNA biomolecular assembly including a) the schematic illustration of the definitions. Reproduced with permission.^[94] Copyright 2017, AAAS. b) Complementary binding of short DNA strands to form DNA bricks. Reproduced with permission.^[301] Copyright 2017, Springer Nature. c) DNA origami involving binding and folding of one long and several short staple strands. Reproduced with permission.^[302] Copyright 2011, AAAS. d) Single-strand DNA folding. Reproduced with permission.^[94] Copyright 2017, AAAS.

its advantages and disadvantages concerning design, error rates, fidelity, and the final size of the structure. For example, DNA origami with a single long strand and several short strands is more readily amenable to software design while single long strand DNA folding is not. In contrast, single long strand DNA has been shown to form some of the largest DNA structures.^[94] Recent trends point to future decreases in the cost of DNA synthesis per base,^[95] which suggests increased availability of assembled DNA origami structures for both basic research and commercial applications. Additionally, recent innovations in synthetic biology^[96,97] offer possibilities for biomolecular modifications of DNA strands as well as the incorporation of dynamic biomolecular circuits that could result in the origami-inspired assembly of more complex and even dynamic nucleotide and protein structures.

DNA origami enables precise molecular positioning and assembly in a parallel manner. For example, it has been reported that 100 trillion probe tiles bearing probe sequences of 20 nucleotide long-single-stranded DNA could be fabricated in one step and these tiles could be used to detect even single molecular hybridization and label-free detection of RNA by atomic force microscopy.^[98] Besides there is the possibility to incorporate stimuli-responsive nucleic acid molecules such as i-motifs and G-quadruplexes to enable reconfigurable origami structures.^[99–101] One of the significant challenges is to extend the applicability of these structures to optical, photonic, and electronic structures by functionalization with nanoparticles and related functional components.^[102–105] Other challenges relate to the limited overall size of DNA assemblies; for example, most origami assembled DNA structures have sizes on the micrometer range or below in at least one dimension, and defects plague the assembly of larger structures. Also, while there have been some promising results, the stability and applicability of DNA origami biosystems at high temperatures, outside aqueous environments, and in charged aqueous solvents needs more detailed investigation.^[106,107]

3. Origami Biosensors

The analysis of the properties of biological organisms and their cellular and sub-cellular components with high spatial and temporal resolution has resulted in the development of a range of optical, electronic, and analytic biosensors.^[108] Once cells are broken apart or lysed, identification and analysis of biomolecules can be efficiently carried out with existing biosensors, but more recently there is a push to enable sensing of biomolecular and/or electrical activity of entire organelles, cells, or organs in-situ.^[109–111] One of the central challenges in this endeavor is that organelles, cells, and organs are 3D, while many chip-based biosensing platforms are 2D.^[112] Hence, much information is lost along the surface area of the cell not in contact with the 2D sensor. Also, it can be very challenging if not impossible to probe 3D spatiotemporal activity in-situ using 2D biosensors. Indeed, as compared to 2D planar geometries, other 3D shapes such as tubular biosensors can show enhanced sensitivity.^[113]

Advances in origami microfabrication methods have opened avenues to produce geometrically complex structures with new or improved intrinsic functionalities for biosensing in a truly

3D manner. For instance, an initially conceived 2D structure can be designed to fold towards the third dimension via specific hinges in order to wrap few or even single cells^[114] and potentially organs. The biological sample can be detected or stimulated using electrodes integrated into the origami structure.^[115] The folded structure could conceivably be also patterned with specific magnetic, optical, or biochemical characteristics to target a unique stimulus or measure a selected response of the biosample in-situ and with high 3D spatiotemporal resolution.^[116] Furthermore, the possibility to integrate these microstructures with other microcomponents on-chip has allowed novel lab-on-a-chip prototypes to enable sensing with high spatial resolution.

Origami biosensors can be broadly classified based on the type of origami assembly principle and their detection modality (Figure 3). Regarding the type of assembly technique, both biomolecular origami or controlled bending of intrinsically strained thin films can be used to create biosensors. With biomolecules, as discussed earlier, folding is driven by molecular strain caused by strong and weak intermolecular forces such as covalent, electrostatic, and solvent-mediated and dispersive interactions. Among molecular folding structures, DNA origami structures have been utilized for biosensing primarily due to their affinity and interactions with other nucleic acids.^[31] For example, DNA origami has been used for biosensing single mRNA molecules that were measured after binding using atomic force microscopy.^[98] The high precision and 3D curvature of DNA origami structures is also important for the creation of tiny elements of biosensors such as nanopores with sizes similar to biological pores in cell membranes^[117] or so-called nanocalipers.^[118,119]

The force required for bending thin film origami biosensors can be derived from the release of mismatch strain typically in bilayers of biocompatible materials such as silicon oxide and silicon dioxide that are deposited by vacuum-based thin-film deposition processes such as thermal or e-beam evaporation or sputtering. This approach has been utilized to assemble shell-shaped (Figure 3a)^[115] or cylindrical biosensors (Figure 3b).^[120] An alternate assembly method utilizes wrinkling (Figure 3c)^[121] or buckling (Figure 3d)^[122] of sensors (either unpatterned or patterned), typically on prestretched or heat shrinkable polymers.

Regarding detection modalities, origami biosensors can be broadly classified based on the optical, electrical, or magnetic phenomena used to measure the physical or chemical characteristics of the biological sample and we describe these in detail below.

3.1. Optical Origami Biosensors

Light-matter interactions provide an attractive biosensing platform to measure properties of samples via microscopy and spectroscopy. Molecular origami provides an attractive means to create static and reconfigurable biosensors due to high selectivity for target molecules including ions, organics, cells, and microorganisms. For example, DNA aptamers can be selected based on high-throughput techniques such as SELEX (systematic evolution of ligands by exponential enrichment) to enable high affinity binding to a variety of target molecules.^[96]

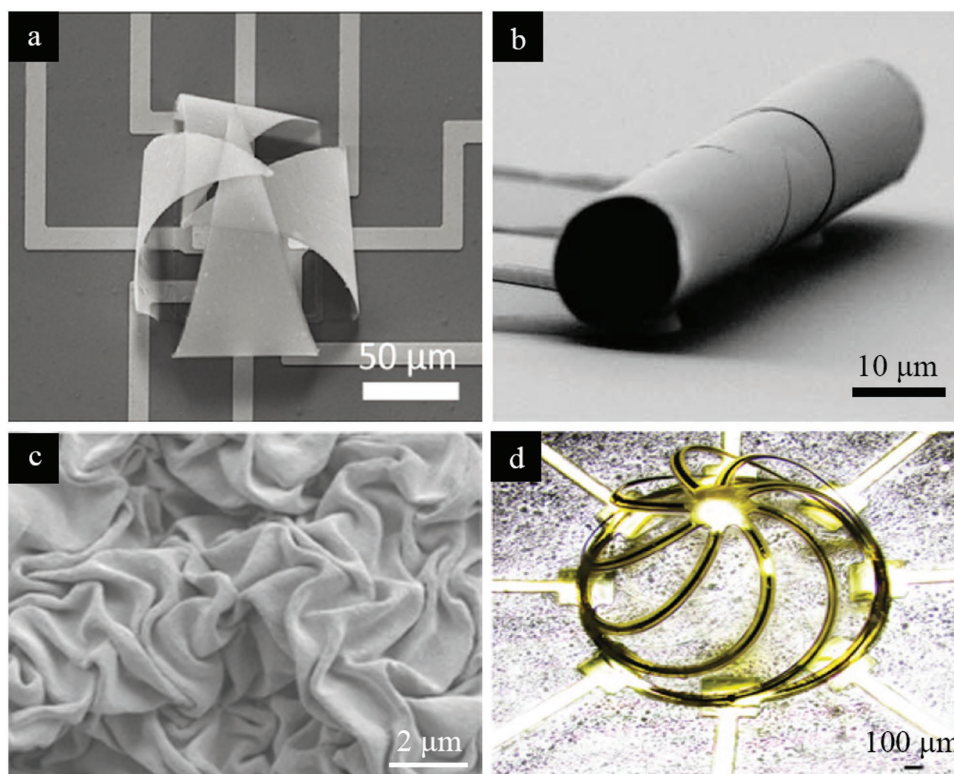


Figure 3. Origami biosensors. a) Self-folding multielectrode shell for recording spatiotemporal electrical responses from live cells. The electrodes on the panels are individually addressable and the shell is transparent, allowing fluorescence imaging. Reproduced under the terms and conditions of the Creative Commons Attribution license 4.0.^[115] Copyright 2018, the authors, published by Wiley-VCH. b) Rolled-up microtube optical biosensor. Reproduced with permission.^[120] Copyright 2012, The Royal Society of Chemistry. c) Wrinkled biosensor. Reproduced with permission.^[121] Copyright 2014, American Chemical Society. d) Buckled cage biosensor with integrated electrodes. The structure has dual functionality as both a culture template and an electrophysiological biosensor of neural cells. Reproduced under the terms and conditions of the Creative Commons Attribution-NonCommercial-NoDerivatives license 4.0.^[122] Copyright 2017, the authors, published by PNAS.

Besides, it has been possible to create assemblies of noble metal nanoparticles to create hot spots for surface-enhanced Raman spectroscopy enhancement^[123–125] or optical nanoantennas that significantly enhance fluorescence.^[126] DNA origami structures have also been used to create molecular rulers based on fluorescence resonance energy transfer rulers^[127] and super resolution microscopy.^[128]

Apart from molecular origami biosensors, thin-film origami has been used to create a range of curved folded biosensors that can elicit new optical effects that are not readily available in planar biosensors. For example, it has been observed that higher order plasmon modes such as quadrupoles provide a crucial advantage of gold patterned cubic versus 2D resonators; these modes can enable low-loss narrow resonances that could increase the sensitivity of plasmonic biosensors.^[129]

Origami also provides new routes to guide light inside microstructures for biosensing. For example, manual or machine-assisted bending of optical fibers can be used to form a u-shaped structure that presents a larger evanescent field at the folded region due to scattering of light.^[130–132] Thus, the transmitted light at the other end of the fiber is influenced by the absorption of light from analytes near the surfaces of the fiber at its u-shaped section and can be utilized for sensitive biosensing. The additional inclusion of noble metal nanoparticles can further enhance sensitivity. With this combined approach,

Sai et al. have found a tenfold improved absorption after coating a bent fiber with a monolayer of gold nanoparticles and could be used to detect sucrose solutions, protein antibodies (anti-Human Immunoglobulin G) via complementary bioreceptors, alpha-fetoprotein, and *Escherichia coli* bacteria.^[130–132]

Rolled-up tubular microstructures based on the release of prestrained nanometer thick membranes are a popular approach to create cylindrical and tubular biosensors.^[37,133–135] Light confined in the tube wall and propagating along its azimuthal direction gives rise to optical resonances, which emerge due to constructive interference of light recirculating inside the closed loop of the origami-assembled microstructure. These optical resonances can be confined in a wide variety of structures with circular symmetry, and are commonly referred to as whispering gallery mode (WGM) optical microcavities.^[136] Depending on the optical characteristics of the microcavity, photoluminescence or transmission spectroscopy is usually employed for biosensing, where the WGMs are identified as sharp peaks in the optical spectrum. Rolled-up tubular microcavities feature efficient confinement of WGMs that is evidenced by high quality factors (Q) of up to 10^3 , which is a figure of merit for WGMs. Q is related to the sharpness of the WGM and is defined as $Q = \lambda/\Delta\lambda$, where λ is the WGM wavelength and $\Delta\lambda$ is the width of the WGM peak in the optical spectrum.

Figure 3b shows a scanning electron microscopy (SEM) image of a rolled-up tubular microcavity. This type of structure features wall thickness at subwavelength dimensions (i.e., smaller than the WGM wavelength). As a result, a large proportion of the WGM field intensity extends out of the tube wall and serves as a probe of the medium in the vicinity of the tube wall. By monitoring changes in the spectral positions of the WGMs it is possible to quantify refractive index (RI) changes and consequently label-free sensing of analytes medium adjacent to the microcavity surfaces.^[120,137,138] These sensors, often referred to as RI optical biosensors, offer extremely high sensitivity as high as 880 nm RIU⁻¹ (RIU: refractive index unit) for phosphate-buffered-saline (PBS) solution with different concentrations of glucose.^[120]

As an alternative to the RI biosensing, Smith et al. have monitored the *Q* factor of WGMs to detect single NIH 3T3 embryonic fibroblast mouse cells in rolled-up tubular microcavities.^[137] They argue that gaps among consecutive windings in the tube walls that occur during the rolling-up process act as optical defects that strongly reduce the *Q* values. When a cell, with a diameter of ≈ 15 μ m, exerts an outward mechanical force on the tube walls, with typical diameters of 10 μ m, the gaps are reduced in size, which results in enhancement of *Q* factors of about two to ten times. Their proposed optical biosensor not only demonstrates a method to detect single cells, but can also be used to determine the mechanical interactions of single live cells.

In addition to tubes, strain engineering has also been utilized to create shell-based sensors for imaging and spectroscopic analysis of the membranes of single cells. The so-called mechanical trap surface enhanced Raman spectroscopy involves wrapping a single cell with a self-folding bilayer patterned plasmonic enhancing nanostructures.^[114] Then using confocal Raman imaging, it was possible to map the lipid and protein moieties on the surface of single cells with 3D spatial resolution.

3.2. Electrical and Magnetic Origami Biosensors

Electric and magnetic phenomena are often used to characterize, record, and stimulate electrical properties of biological samples. Origami methods allow the fabrication of electrical and magnetic biosensors with interesting geometrical features and enhanced sensing responses. For instance, flexible planar carbon electrodes functionalized for the detection of glucose molecules show an increased electrical response of up to 125% after being manually bent.^[139] In another example, origami has been employed to bend planar microelectrodes that contain a nanoscale field-effect transistor (nano-FET) tip at the folded-end of the electrodes. In this way, the nano-FET tip acquired a free-standing characteristic and could enter into single cardiomyocytes and record their intracellular potentials and beating activities.^[140]

Rolled-up architectures have been widely used for biosensing. One strategy consists of releasing pretrained bilayers with integrated electrodes that self-assemble into 3D microstructures with tailored functionalities.^[115,141] With this approach, impedimetric biosensing was used to detect biosamples ranging from HeLa or lymphocyte cells scales down to DNA molecules.^[113,141,142] The sensing performance of these origami biosensors has been reported to be two to fourfold enhanced as compared to their planar analogs due to higher

electric fields and compactness among cells and electrodes imposed by the tubular geometry.^[113,141,142] It is important to note that the hollow core feature of these tubular geometries is advantageous to couple them with microfluidic components, allowing their use as impedance-based flow cytometers that are capable to detect single cells in real time and label free.^[113,141,142] Ger et al. have demonstrated a magnetic origami biosensor self-assembled by rolling up a magnetic film that actively attracts cells containing diluted magnetite (Fe₃O₄) nanoparticles.^[143] Further electrical, photonic, and magnetic features could be potentially integrated on different sections along these rolled-up microstructures,^[144–148] promoting them as lab-in-a-tube biosensing devices.^[116,149] Elsewhere rolled-up geometries based on polymers or rolled-up meshes have been utilized for biosensing. Examples include, self-rolling gradient crosslinked epoxy SU8 film coated with graphene,^[150] and rolled-up macroporous nanoelectronic networks and mesh nanoelectronics for electrical biosensing.^[151,152] In addition to rolled-up geometries, multifingered grippers patterned with individually addressable electrodes have been used to trap even single cells^[153] and measure electrical activity from few neonatal rat ventricular cardiomyocytes (Figure 3a).^[115] As reported in the paper, by wrapping the cells with individually addressable electrodes it is possible to gain significantly higher signal-to-noise ratios as compared to planar sensors, but also enable 3D spatiotemporal activity of electrogenic activity.

Mechanical buckling origami approaches have also been employed to fabricate self-assembled wrinkled electrodes with multiscale features all the way from millimeter to nanometer scales. These 3D electrodes are shaped by heat shrinking of elastomeric substrates with previously patterned planar electrodes.^[121,154,155] A direct consequence of the buckling process is an increase of the surface area to volume ratio, which improves the performance of these electrodes as biosensor units when compared to their planar counterparts.^[156] Figure 3c shows a top-view SEM image of a wrinkle electrode with a miniaturized surface area of about 84% after the shrinking process. These electrode biosensors have been proved to be sensitive to DNA molecules and glucose by employing electrocatalytic measurements.^[121,155]

Controlled compressive buckling offers an alternative strategy to build 3D mesostructures with predetermined intricate shapes that pop out from a 2D design.^[49,122,157–160] Yan et al. have used this approach to fabricate a 3D cage (made of epoxy (SU-8)),^[122] as depicted in Figure 3d. They integrated a microelectrode on the outer surface of each leg of such 3D cages by patterning gold micropads of 50 μ m in diameter. The final device was used as an electrical biosensor and a 3D cell scaffold for growing neural networks of dorsal root ganglion (DRG) cells. Through the integrated electrodes, they explored the electrophysiological activity of the DRG neurons by electrically stimulating them and then recording their action potential responses in real time, which were consistent with the readings reported for typical 2D electrode structures.

4. Origami Microfluidic Devices

Mimicking the complex microfluidic networks in biological systems is not only critical for lab-on-a-chip, organ-on-a-chip, and

related high-throughput in vitro biosystems, but also for tissue engineering and regenerative medicine.^[4,161–163] For high-throughput analysis, the integration of additional components, like electrodes or optical waveguides, opens new functionalities for bioanalysis.^[164,165] Origami techniques can enable placement of microfluidic channels and functional modules in 3D architectures and curvilinear geometries. In organ-on-a-chip applications,^[166] there is a need to replicate human vascular networks in three dimension. One of the issues in conventional microfluidics is that fluidic channels have a rectangular cross-section while fluidic channels in the body have circular cross-sections, and this can be mimicked in roll-up technologies. Besides, origami approaches can enable curved and folded fluidic networks reminiscent of those in human organs, which is an advantage over 3D printing that requires the use of sacrificial materials and has limited resolution at small size scales and in folded geometries.^[167,168] We discuss major classes of origami microfluidics based on their applicability for bioanalysis or biomimicry.

Concerning bioanalysis, with the introduction of microfluidic paper analytical devices (μ PADs),^[166,169] the control of liquids in 3D was achieved by stacking 2D layers of paper-based microfluidic platforms.^[169] In these systems, the hydrophilic characteristic of paper ensures liquid flow via capillary action without the need of external pumps, and fluid distribution is controlled by channels and reservoirs patterned on each paper layer with photoresist or wax, which repel liquids due to their hydrophobic characteristics.^[170] Liu and Crooks have described a method to assemble 3D μ PADs based on origami principles, where the stacking of 2D paper layers was achieved by sequences of hand-folding of a single sheet of paper without the need of alignment methods.^[171] Other exciting origami biosystems have been reported following this assembly methodology where electrodes can be integrated and are activated by the folding process.^[172–185] **Figure 4a** shows a photograph of an unfolded 3D μ PAD device demonstrating the distribution of four colored solutions among nine paper panels that are folded into the 3D microfluidic μ PAD. External clamps hold the assembled layers tightly and drops containing 10 μ L of solution added on the top layer diffuse for 5 min before the device is unfolded. The microfluidic networks were patterned via an inexpensive photolithography process without the need of clean room facilities, with reservoirs of 2.5 mm in diameter and channels of 900 μ m wide and 100 μ m thick, which was predetermined by the thickness of the paper. They employed this 3D origami-assembled μ PAD to flow and detect

solutions containing glucose and bovine serum albumin (BSA). Multiplexed analysis at different layers could be readily achieved by unfolding the origami μ PAD. Some reservoirs in the paper layers were modified for specific colorimetric reactions that were qualitatively interpreted by the naked eye or quantified by image intensity analysis, achieving a detection limit of 0.14×10^{-6} M for BSA.

Origami techniques can produce microchannels with cross-sections and dimensional features that resemble biological vessels and capillaries. Some examples include circular-shaped (Figure 4b)^[137] or irregular triangle-like (Figure 4c)^[186] microchannels with wall thickness below 1 μ m and self-assembled via folding processes. Additionally, origami approaches have been used to create wrinkled-up nanochannel networks that are otherwise challenging if not impossible to produce using traditional soft-lithography methods.^[37,187,188]

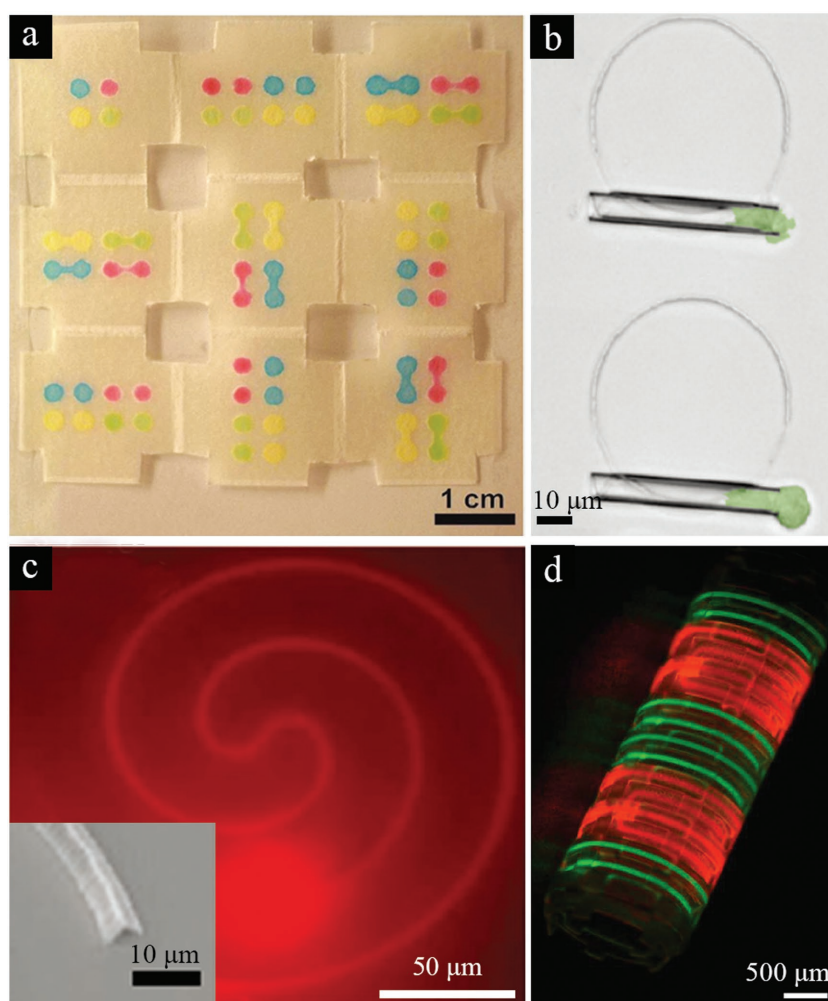


Figure 4. Origami microfluidics. a) An unfolded 3D paper origami microfluidic device (3D- μ PAD). Reproduced with permission.^[171] Copyright 2011, American Chemical Society. b) Lab-in-a-tube as a microfluidic channel for single-cell analysis. Reproduced with permission.^[137] Copyright 2011, American Chemical Society. c) Self-folded triangular-shaped microchannels. The inset is the corresponding SEM image of one end of the channel. Adapted with permission.^[186] Copyright 2017, Wiley-VCH. d) Rolled-up integrated microfluidic dual-channel device with PDMS fluidic layer and self-folding gradient cross-linked SU8 layer. Reproduced with permission.^[74] Copyright 2011, Macmillan Publishers Limited.

These self-assembled microstructures can be adapted to work with conventional (rectangular cross-section) microfluidic channels.^[113,120,189] Accordingly, tubular microchannels, with their built-in hollow feature, can be coupled to typical microchannels whereby small volumes of glucose and PBS solutions (1–2 μL),^[120] or solutions with cells (Jurkat T lymphocytes 1.2×10^6 cells per milliliter) flowed.^[113] As shown in Figure 4b, these tubular microtubes, with a diameter of $\approx 10 \mu\text{m}$ and a wall thickness of $\approx 200 \text{ nm}$, were also used as microchannels for pumping of cells with even larger cross-section areas (up to 2.3 times larger).^[137] In this work, cells were sucked in and out of the tubular microchannels by an external capillary tip placed at one end of the tube. As we pointed out in the previous section, the roll-up origami technology can produce self-assembled tubular microstructures with functionalized photonic or magnetic characteristics and integrated electrodes, so that these microchannels can be explored as lab-in-a-tube microfluidic biosystems.^[116,149]

Origami is an appealing strategy to create out-of-plane curved microchannels to mimic 3D microfluidic networks found in nature such as leaves, tissues, and insect wings. Thus, manual rolling of 2D polydimethylsiloxane (PDMS) microfluidic devices

has been utilized to create bent channels ($300 \times 300 \mu\text{m}$ cross-section) that facilitate fluid mixing.^[190] Other approaches to fabricate curved 3D microfluidic platforms rely on strain engineering principles. In one example, Jamal et al. used gradient UV crosslinking of SU-8 films to create a swelling gradient in the film so that it curved through a de-solvation process in water.^[74] PDMS microchannels were integrated onto the SU-8 films before self-rolling the 3D microfluidic structures, with an overall PDMS/SU-8 thickness below $40 \mu\text{m}$. Figure 4d exhibits a 3D curved microfluidic device created with this approach and used to flow fluorescein (green) and rhodamine B (red) in dual-channel devices.

5. Cell and Tissue Engineering

Tissues and organs are self-organized 3D micro to macrostructures many of which are curved and folded with large organ and species diversity and sizes including millimeter to centimeter wrinkles on hornbeam leaves,^[191] spinules of the dorsal skin of some geckos with a spacing of around 400 nm ,^[192,193] intestinal villi and gyri and sulci on the cerebral cortex (Figure 5a–d).^[194–196]

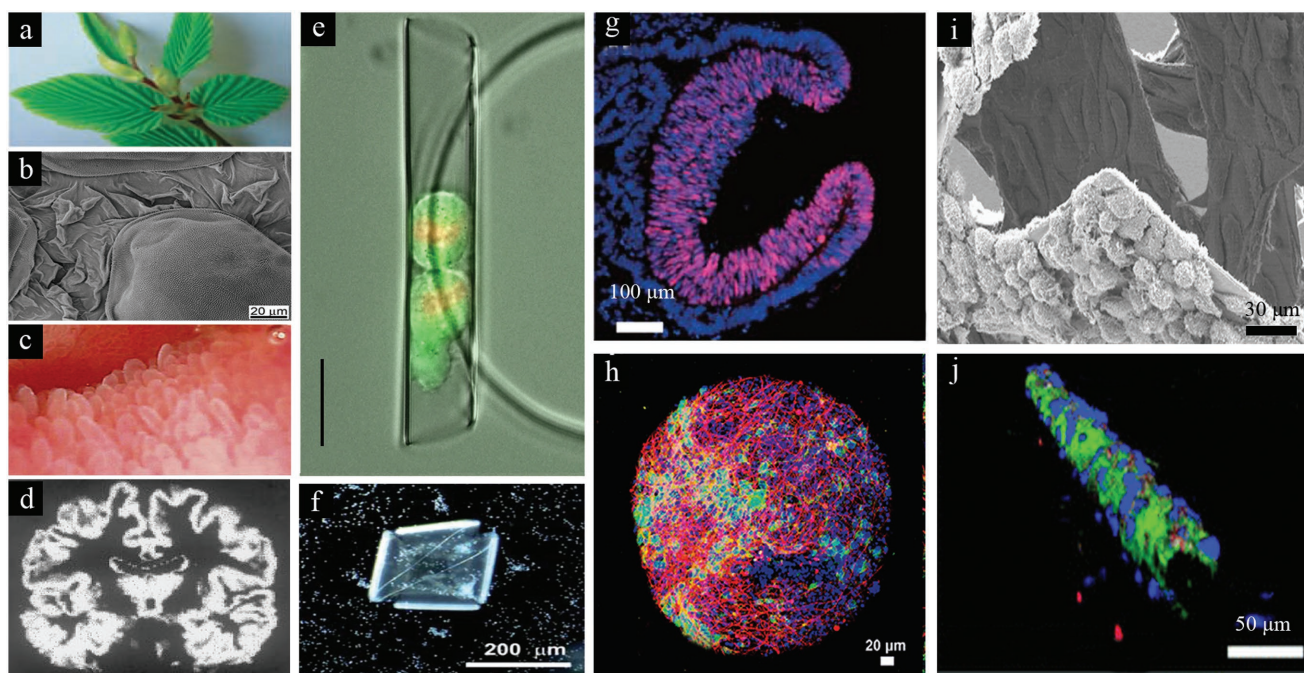


Figure 5. Origami cell and tissue engineering. a–d) Naturally occurring curved and folded structures including hornbeam leaf, gecko skin, villi, and brain folds. a) A photo of hornbeam leaves with blossom buds, (length, 5 cm). Reproduced with permission.^[191] Copyright 2005, AAAS. b) SEM image of gecko epidermal dome skin regions, with microbucklings between the dorsal regions. Reproduced with permission.^[193] Copyright 2015, Elsevier. c) Video endoscopic image of normal duodenal villi after water instillation. The villi are regular and ordered finger-shaped with fine patterns. Reproduced with permission.^[194] Copyright 2004, American Society for Gastrointestinal Endoscopy. d) Segmented grey matter fold images from optimized value based management (VBM) technology. Reproduced with permission.^[196] Copyright 2001, Elsevier. e) Fluorescent and phase contrast images of HeLa cells encapsulated in rolled-up tubes during the cell division process. The green color indicates GFP tubulin and the red color H2B-mCherry. The scale bar is $15 \mu\text{m}$. Reproduced with permission.^[212] Copyright 2014, American Chemical Society. f) Dark field image of a self-folding cell encapsulation device, encapsulating yeast cells in thermoresponsive hydrogel bilayers. Reproduced with permission.^[217] Copyright 2011, The Royal Society of Chemistry (RSC) on behalf of the European Society for Photobiology, the European Photochemistry Association, and the RSC. g,h) Stem cell derived organoids. g) Dark field image of self-formed optic cup structures from 3D cultured embryonic stem cells. Adapted with permission.^[219] Copyright 2011, Springer Nature. h) Optical image of a human 3D brain microphysiological system (BMPS) after 8 weeks of differentiation. Adapted under the terms and conditions of the Creative Commons Attribution license 4.0.^[221] Copyright 2015, the authors. i,j) Cell culture on rolled-up and self-folded tissue scaffolds. i) SEM image of self-folding tissue scaffolds, with cells attached on both the inner and outer walls of the scaffolds. Reproduced with permission.^[226] Copyright 2010, Elsevier. j) Confocal image of endothelial cells in porous self-folded tubular tissue scaffolds. The nuclei are stained blue and actin is stained green. Adapted with permission.^[236] Copyright 2015, The Royal Society of Chemistry.

The disruption or absence of folds in organs such as the brain can have devastating developmental consequences. Examples of such diseases include ulegyria (distortion of gyri due to the scarring in the deep regions of sulcus)^[197,198] and lissencephaly (smooth brain without gyral pattern).^[199,200] In addition to the unique folded shape of the 46 final structure, several key events in embryogenesis themselves involve curving and folding driven by processes such as apical contraction, apico-basal contraction, or basal expansion of epithelial cell sheets. These processes cause invagination involved in gastrulation leading to the final structure of the gut or neurulation resulting in the formation of the neural tube that eventually differentiates into the brain and spinal cord.^[62,201] Apart from intrinsic cellular changes, external forces or pressure can also form folds in epithelia, which has been attributed as a potential morphogenetic mechanism for formation of the folds in the ciliary body of the avian eye.^[202]

Hence, it is natural to investigate strain engineering processes to develop tissue mimics for both in vitro studies and in vivo tissue engineering. Also, when cells are cultured beyond flat Petri dishes, notable differences arise including morphological, growth rate, gene expression, and drug sensitivity.^[203–209] For example, decades ago it was shown that interferons, which are immune modulators, are less efficient at inhibiting tumor growth in 3D spheroids as compared to monolayer culture.^[210] Elsewhere, researchers observed significantly lower antiproliferative effects of cancer drugs such as doxorubicin, paclitaxel, and tamoxifen as well as differential gene expression profiles in 3D models as compared to monolayer MCF-7 cancer cell culture.^[204] These examples represent a small subset of a large number of studies showing marked differences between 3D and 2D cell culture models, and there is now an overwhelming consensus that there is a need to create 3D platforms that more accurately mimic cell behaviors in-vivo.^[208,211]

Transparent rolled-up tubes based on strain engineered thin films provide an attractive means to observe single-cell behavior in confined spaces. In single-cell studies using both transformed (HeLa) cancer cells and nontransformed retinal pigment epithelial cells (RPE1), spatial confinement had dramatic consequences on mitotic progression and caused chromosomal instability as compared to free cells (Figure 5e).^[212,213] While there have been numerous studies on cell confinement in conventional microfluidic channels, they have been done predominantly in rectangular cross-sectioned microfluidic channels made using planar photo or soft lithography. Rectangular cross-sectioned channels feature inhomogeneous curvature with flat surfaces and cornered edges that can alter cell behavior and fluid flow.^[214,215] This rectangular cross-section is quite unlike the circular cross-section of vascular conduits such as blood vessels in vivo,^[214–216] and these homogeneously curved and round cross-sectioned fluidic channels are better mimicked by rolled-up microtubes.

Elsewhere, cells have been encapsulated in thermoresponsive self-folding biodegradable polymers for potential cell therapy applications (Figure 5f).^[217] In one report, the authors claim that a rolled-up biodegradable hydrogel device that encapsulates cardiac cells and supports viability could potentially be delivered in a compact form via a catheter and the devices would unroll and expose cells to the impaired myocardium.^[218]

In addition to in vitro systems, curved and folded tissue constructs are being explored to create more anatomically accurate tissue engineering models. Indeed, studies in stem cell tissue morphogenesis show progressive curving following invagination of embryonic stem-cell-derived retinal epithelium to form the optic cup shape after about 10 d in culture (Figure 5g).^[219] More recently, a number of studies have demonstrated the formation of curved organoids in stem cell culture including a self-organized kidney,^[220] and human brain microphysiological systems (BMPS) (Figure 5h).^[221] In BMPS, synaptogenesis, neuron-to-neuron, and neuron-to-glial interactions increased after eight weeks of differentiation. These curved and folded organoids offer significant promise for investigating diseases, toxicity, drug discovery, and regenerative medicine.^[221–223]

Strain engineering based on self-rolling methods has been used to create a variety of 3D curved tissue scaffolds. These include single and multilayered rolls (Figure 5i,j)^[224–235] and vascular mimics.^[236–238] They highlight the advantages of origami approaches such as facile layering of different cells and matrix as is needed in several tissues including blood vessels, the ability to leverage state of the art 2D patterning techniques such as photopatterning, contact printing and soft-lithography, and the ability for high-throughput fabrication of curved and folded cellular geometries that can be hard to access by other methods. Also cells cultured in curved geometries can display dramatically different behavior as compared to flat structures. For example, both basal and stimulated insulin production was observed to be significantly higher from β -TC6 insulinoma cells cultured in self-rolled tubes as compared to those cultured on a flat substrate over a period of approximately two months.^[230] They highlight the need for origami cell culture systems, where structures can be produced in a highly parallel manner with micropatterns in curved and folded geometries. Besides, it has recently been reported that cells themselves could potentially fold structures based on cell traction forces.^[239] This report highlights the possibility to create complex hybrid cell-microstructure bionic devices and microtissues as well as to measure cell traction forces.

6. Drug Delivery Biosystems

Drug delivery has evolved from powder or liquid formulations to multifunctional complex shaped nanoparticles to patch-based delivery systems aimed at enhancing tissue targeting, enhancing bioavailability, and reducing side effects.^[240,241] Origami can augment the capabilities of present-day drug delivery systems by enabling stimuli-responsive folding, bending, and curving of complex 3D shapes of importance in encapsulation, retention, and release of drugs (Figure 6). Origami drug delivery biosystems can be broadly classified into (a) self-folding capsules that can encapsulate or release drugs either permanently or when triggered by a stimulus such as pH, temperature, or biomolecules, and (b) self-gripping patches. It is noteworthy that there are also motile and reconfigurable systems of relevance to drug delivery and these are discussed in the following section on biorobotics.

Molecular folding can provide an attractive means to create nanoscale static and reconfigurable nanostructures for

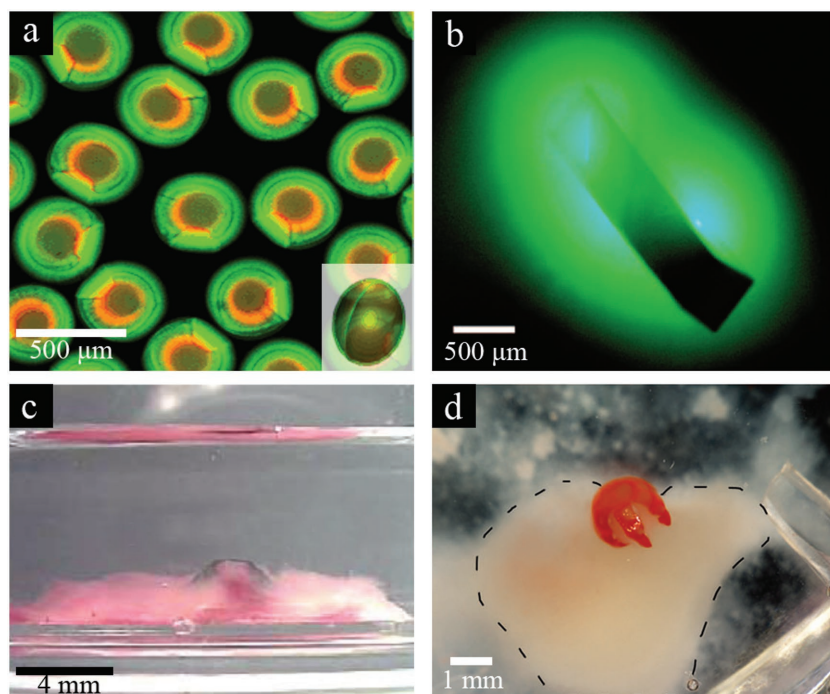


Figure 6. Origami drug delivery systems. a,b) Self-folded spherical and polyhedral capsules. a) Confocal microscopy image of self-folded spherical microcarriers composed of hydrogel bilayers. Reproduced with permission.^[250] Copyright 2012, Wiley-VCH. b) Optical fluorescence image showing release of fluorescein in a helical spatial pattern. Reproduced with permission.^[252] Copyright 2011, Wiley-VCH. c,d) Self-folded patches and theragrippers. c) Image of a bilayer self-folding hydrogel patch releasing a blue dye on mucus. Adapted with permission.^[263] Copyright 2006, Elsevier. d) Optical image of a doxorubicin loaded self-folded theragripper gripping onto a clump of cells. Reproduced with permission.^[264] Copyright 2014, Wiley-VCH.

delivery of drugs. For example, DNA origami drug delivery vehicles have been utilized for delivery of doxorubicin to cancer cells, and there are reports that these DNA origami based conjugates result in a greater reduction of tumor size over the same time as compared to bare drug in in-vivo mice models.^[242,243] Self-assembly of short strands of DNA into polyhedra such as icosahedra and tetrahedra has resulted in the development of a range of drug carriers. In one report, siRNA-hybridized DNA tetrahedra were shown to have longer circulation times in-vivo as compared to the bare siRNA.^[244] Several advantages of DNA origami nanostructures for drug delivery have been noted. These include the possibility for high drug loading, targeting using aptamers, the slow degradation that reduces unintended release, and tailored size/morphology.

At larger length scales, surface tension,^[245] stress,^[246] or swelling^[247] driven bending and folding have been used to encapsulate a range of drugs and cells.^[248,249] Regarding shapes, a variety of configurations have been explored including oblate spheroids,^[250] tubes,^[217,251] and polyhedra.^[252] These include permanently bonded polyhedral capsules sealed with biocompatible polymers such as polycaprolactone (PCL)^[245] or reconfigurable structures composed, for example, of stimuli-responsive polymers such as *N*-isopropylacrylamide.^[250] An attractive feature of self-folding capsules is that they can be precisely patterned with a range of pore sizes, densities, and patterns that can permit 3D spatiotemporal release with unprecedented control. For example, as

depicted in Figure 6b, chemical release profiles in a helical spatial pattern can be realized and such spatial chemoattractant patterns were used to organize bacteria cells in a helix.^[252] Elsewhere, precise nanopores patterned on self-folding polyhedra were utilized to package cells for cell encapsulation therapy; the 3D patterns permit higher diffusion of nutrients as compared to planar membrane capsules while offering the possibility for immunoisolation based on size exclusion.^[253,254]

Surface tension based microfolding of thin films builds on principles involved in liposomal self-assembly that results in curved capsules for drug delivery, which can enhance drug loading, bioavailability, and targeting. For example, the solubility limit of transporting amphiphilic and lipophilic drugs such as acyclovir and insulin in the blood can be overcome by liposomal capsules.^[255,256] Liposomes can also specifically target cell membranes and release the drugs under specific stimuli such as pH,^[257] light,^[258] or temperature changes.^[259,260] Through this process, vast amounts of drug can be delivered to the targeted position, which can increase the delivery efficiency dramatically. Thin film capsules, like liposomes, can form spontaneously due to minimization of surface-free energy but with the additional advantage that they can be precisely patterned using planar lithography approaches.

Drug delivery patches such as transdermal or buccal patches offer the possibility for sustained release of drugs over long periods of time. These patches typically contain an adhesive and drug-eluting layer and can be applied for local or systemic drug delivery. While transdermal and buccal patches can be applied manually, there is a need for patches for other regions of the body such as the gut and intestine for delivery of drugs for a range of diseases such as diabetes, hepatitis, and cancer. With this tight adhesion, the leakage of drugs is reduced and the bioavailability is increased. In fact, the amount of model drugs absorbed from intestinal patches can be several fold higher than that from solution.^[261] Self-rolling bilayers have been used to create unidirectional patches for drug release. These systems were composed of a self-rolling pH responsive bilayer, mucoadhesive, and enteric coating.^[262,263] In order to enhance the gripping characteristics, more recently, so-called multifingered therapeutic grippers or theragrippers have been developed. Apart from the multifingered shape and sharp tips, the theragrippers are composed of a stiff polymer coupled with a swellable stimuli-responsive hydrogel so that it can grip firmly into the mucosa. The theragrippers have been used for delivery of dyes in vivo and drugs such as doxorubicin to cells in in vitro culture. It was observed that a greater fraction of cells died with a theragripper patch as compared to an unpatterned bilayer patch.^[264] Still, significant challenges exist in design, biocompatibility, biodegradability, and retention of thin-film origami drug delivery systems.

7. Origami Biorobotics

Origami approaches can enable the creation of complex 3D robotic structures by utilizing hinges and smart actuators that can bend and straighten out in response to wired inputs or environmental stimuli.^[56] Origami biorobots offer advantages of a top-down assembly process starting from a flat, composite layer/sheet that can have multiple degrees of freedom. Planar technologies such as photolithography, rapid prototyping, and additive manufacturing can be used to pattern the sheet. Besides, rigid and soft materials can be included to adjust the compliance and tune local stiffness to accomplish specific shape changes and tasks.^[56] Other functional units can be integrated into self-folded biorobots for locomotion, power, and external communication. In many cases, origami biorobots can resemble shapes and scaffolds of biological systems and mimic functions optimized beyond the capabilities of hard robots. For example, shape change can overcome obstacles and apply smaller forces required for biomedical operations. Origami robots can include distributed pneumatic networks or hydraulic actuators in combination with soft, conductive, and optically transparent materials, providing new mechanisms for their movement, control, and manipulation.^[265] Origami biorobots can be broadly classified into shape-change bioimplants, rolled-up micromotors, and folded grippers and sheets. These are detailed below.

7.1. Origami Shape-Change Bioimplants

Dramatic changes in shape can occur during flat and deployed states of origami that provide significant advantages for packaging and deployment of implants.^[54] For example, 3D intracardiac magnetic resonance imaging coils can significantly enhance the signal-to-noise ratios as compared to surface coils and researchers have demonstrated catheter deployable basket and tetrahedron-shaped imaging loop coils.^[266] Elsewhere, origami designs based on thermally activated shape memory alloys have been utilized for self-deploying stent grafts.^[267] More recently, the shape change of 3D printed structures also referred to as 4D printing, is being utilized to personalize biomedical devices with a wide range of applications. For example, endoluminal stents have been 3D printed based on digital models of the trachea using methacrylated PCL and these structures can undergo an expansion based on a shape memory effect.^[268]

7.2. Tubular and Helical Micromotors

Human-made micromotors have been inspired by motile cells such as bacteria that can effectively move at very low Reynolds numbers at speeds greater than that enabled by Brownian motion.^[269–271] Similar to biological systems, synthetic micromotors represent a new class of human-made chemo-mechanical systems, which convert local chemical energy and/or energy of external fields into motion.^[41] A variety of different propulsion mechanisms of synthetic micromotors have been reported including motion driven by

self-electrophoresis, self-diffusiophoresis, interfacial surface tension, fluid pumping, and bubble recoil. One popular class of origami-inspired micromotors involves so-called tubular microengines. These motors are fabricated by the release of strain engineered 2D nanomembranes by selective etching of an underlying sacrificial layer and can be composed of a range of materials including soft polymers, hydrogels, metals, semiconductors, and ceramics.^[37,272] In addition, by inclusion of a catalyst such as platinum (Pt) only on the inside of the tube, micromotors can be designed so that chemical decomposition of fuel such as hydrogen peroxide takes place only inside the tubular microcavity. This design results in bubble propulsion and ultrafast speeds observed to be around ten times higher than state-of-the-art self-electrophoretic and self-diffusiophoretic nano/micromotors.^[273] Besides, it has been observed that tubular microcavities enable better control over bubble generation, reaction–diffusion processes, and gaseous oxygen supersaturation during the decomposition of the hydrogen peroxide fuel into oxygen and water.^[274] Microtubes with the catalyst Pt deposited on stimuli-responsive polymer bilayers were shown to be capable of moving and progressively changing shape.^[275] Regarding, functionality, rolled-up catalytic micromotors can also be created with unique shapes such as sharp tapered ends so that they can function as nano or microscale tools and penetrate into even a single cell or into tissue (**Figure 7a**).^[276,277] These and other examples demonstrate the applicability of untethered externally powered and catalytic origami-based micromotors for biomedical applications such as drug delivery and minimally invasive surgery.^[278–282]

Apart from microtubes, other common externally propelled micromotors include flagella inspired helical microrobots capable of moving in wobbling or corkscrew motions.^[283,284] The so-called artificial bacterial flagella have helical shapes constituted, for example, with a soft magnetic head composed of Cr/Ni/Au and a self-coiling InGaAs/GaAs/Cr tail.^[285] Due to the helical shape, these micromotors can be moved by rotating magnetic fields as opposed to field gradients, which enhances applicability in vivo. In addition to motion of microhelices on their own, they can also be coupled to larger objects to aid in propulsion or steering. For example, magnetic microhelix hybrids have also been created and used to capture, transport, and deliver immotile live spermatozoa to an oocyte.^[286]

7.3. Flat Sheet, Buckled, and Gripper-Based Biorobots

Flat sheets can be patterned using self-folding hinges to create multifunctional robots that can be deployed in a compact state and unfold on entry into the body. An example is an ingestible, controllable, and degradable origami robot designed for noninvasive clinical interventions, such as removing swallowed batteries or patching stomach wounds (**Figure 7b**).^[287] The robot consists of laminated biodegradable drug-eluting sheets encapsulated in ice for robot delivery. The sheets also include a heat-sensitive shrink film for self-folding. The origami design was based on its ability to fold into a compact shape so that it could be introduced into an ice capsule. In in-vitro studies, the researchers observed that as the ice melted, the robot unfolded

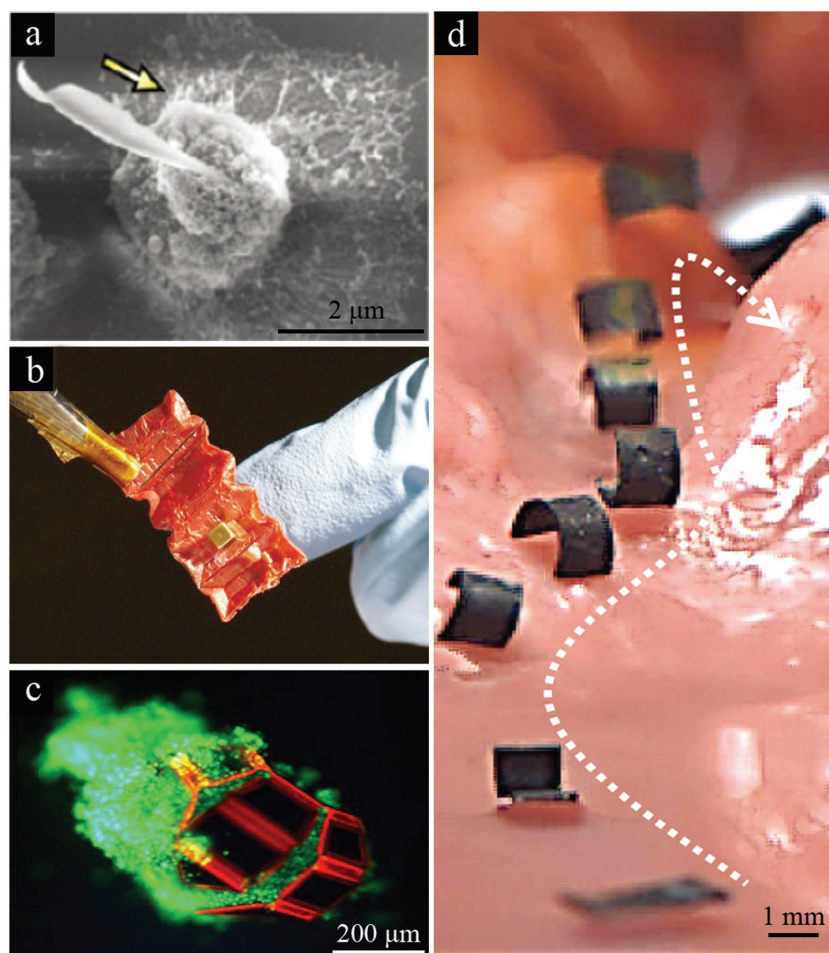


Figure 7. Origami biorobotics. a) SEM image of a rolled-up sharp self-propelled tool piercing into a single paraformaldehyde fixed HeLa cell. Reproduced with permission.^[276] Copyright 2012, American Chemical Society. b) Origami inflatable robot composed of pig skin and self-folding shape. Reproduced with permission.^[287] Copyright 2016, IEEE. c) Thermobiochemically actuated microgripper with live excised L929 fibroblast cells retrieved in biopsy experiments on a cell clump. Reproduced with permission.^[289] Copyright 2009, The National Academy of Sciences of the USA. d) Magnetically propelled multimodal locomotion of a soft robot across a stomach phantom. Adapted with permission.^[295] Copyright 2018, Springer Nature.

and adopted a flat state. When a neodymium magnet was incorporated, the structure could also be controlled and guided by magnetic fields.

Elsewhere, free-standing buckled structures have been coated with platinum to enable bubble propulsion, and it was shown that the trajectory could be controlled based on shape.^[122] Buckling mechanisms can also induce variable stiffness in structures of importance to biorobotics. An example is an origami structure composed of torsional shape memory alloy actuators that can change from a flexible to stiff state via a buckling effect.^[288]

Another class of origami biorobots includes thermobiochemically actuated untethered microgrippers,^[289] of relevance to drug delivery and minimally invasive surgery. They can be composed either of biocompatible metals or biodegradable polymers and hydrogels. For metallic grippers, controlled folding is a consequence of the release of residual stress in bilayer metal hinges. A thermosensitive polymer or wax layer can trigger folding so

that grippers are flat outside the body and fold only when reaching room temperature. These grippers have been utilized in pig models for biopsy and drug delivery.^[264,290,291] In these experiments, a vial composed of tens to hundreds of submillimeter-sized grippers was deployed using endoscopes into the gastrointestinal tract including the esophagus, colon, stomach, and bile duct. These grippers were shown to be successful in biopsying tissue from hard to reach places such as the bile duct^[291] and achieve statistical sampling of large organs such as the colon.^[290] The biopsy process was entirely biocompatible, and cells retrieved were alive (Figure 7c), and it was possible to extract histological, cytological, and genetic information from the samples. Also, the use of thermal cues offers the possibility for autonomous responses and researchers have been investigating the development of similar gripper-like structures that bend and fold in response to pH^[292] or other biochemical cues such as enzymes^[293] or even specific DNA sequences.^[294]

One of the challenges in origami biorobots is the ability to guide and move them in predetermined paths while displaying a range of motions. Recently, external manipulation has become a significant focus in origami biorobotics. For example, a magnetically propelled curved robot made of thin silicon elastomer (Ecoflex 00–10) with hard magnetic neodymium-iron-boron particles was shown to exhibit multimodal locomotion including rolling, walking, jumping, and crawling.^[295] Magnetic micromanipulation coupled with visual or ultrasound feedback has also been utilized to move soft microgrippers to achieve a range of tasks such as avoidance of obstacles or pick and place.^[296,297]

8. Conclusions

In summary, origami-inspired curving and folding of molecules and thin films provide significant new capabilities and functionalities for biosystems. By leveraging planar patterning processes and static or reconfigurable extension into the third dimension, they enable the creation of truly 3D systems that are critical for biological applications. Significant advances have been made and discussed in this review that includes unprecedented and highly parallel 3D micro and nanofabrication of complex structures; stimuli-responsive and multifunctional drug capsules capable of delivering drugs with complex spatiotemporal patterns; curved, tubular, and folded meshes for biosensing; and biologically inspired folded tissue scaffolds and compact miniature robots.

Future challenges exist. For example, the yield, precision, and reproducibility of origami-synthesized structures need

to be carefully measured and optimized. For in vivo applications, biocompatibility and biodegradability are critical for safe implementation. In addition, some approaches such as remote magnetic guidance or manipulation may prove challenging to implement in the 3D human body and new large-scale magnetic platforms need to be developed. New strategies to harvest energy in vivo need to be explored; in this regard, relatively omnidirectional and electrically small antennas have been fabricated using origami approaches.^[54,298,299] None of these challenges seem insurmountable and it is clear that this multidisciplinary field involving scientists, engineers, and clinicians holds significant future promise.

Acknowledgements

V.A.B.Q. and H.Z. contributed equally to this work. D.H.G. acknowledges the Fudan Fellowship Program and the US National Science Foundation Grants DMR-1709349 and CMMI-1635443. Y.M. thanks the support from the Science and Technology Commission of Shanghai Municipality (17JC1401700) and the Changjiang Young Scholars Program of China.

Conflict of Interest

The authors declare no conflict of interest.

Keywords

bio-MEMS, biosensors, drug delivery, minimally invasive surgery, robotics, self-folding

Received: July 27, 2018
Published online: September 5, 2018

- [1] D. W. Thompson, *On Growth and Form (Canto)*, (Ed: J. T. Bonner), Cambridge University Press, Cambridge, UK **1992**.
- [2] P. Ball, *Nature's Patterns: A Tapestry in Three Parts*, Oxford University Press, New York, NY, USA **2009**.
- [3] E. K. Sackmann, A. L. Fulton, D. J. Beebe, *Nature* **2014**, *507*, 181.
- [4] S. N. Bhatia, D. E. Ingber, *Nat. Biotechnol.* **2014**, *32*, 760.
- [5] P. B. Kruskal, Z. Jiang, T. Gao, C. M. Lieber, *Neuron* **2015**, *86*, 21.
- [6] O. S. Fenton, K. N. Olafson, P. S. Pillai, M. J. Mitchell, R. Langer, *Adv. Mater.* **2018**, *30*, 1705328.
- [7] G. M. Whitesides, *Angew. Chem., Int. Ed. Engl.* **2018**, *57*, 4258.
- [8] P. Gutruf, J. A. Rogers, *Curr. Opin. Neurobiol.* **2018**, *50*, 42.
- [9] F. H. Martini, J. L. Nath, E. F. Bartholomew, *Fundamentals of Anatomy & Physiology, Global Edition*, Pearson Education Limited, Harlow, UK **2016**.
- [10] V. F. Puentes, K. M. Krishnan, A. P. Alivisatos, *Science* **2001**, *291*, 2115.
- [11] G. M. Whitesides, B. Grzybowski, *Science* **2002**, *295*, 2418.
- [12] J. C. Love, L. A. Estroff, J. K. Kriebel, R. G. Nuzzo, G. M. Whitesides, *Chem. Rev.* **2005**, *105*, 1103.
- [13] J.-M. Lehn, *Eur. Rev.* **2009**, *17*, 263.
- [14] A. Ulman, *An Introduction to Ultrathin Organic Films: From Langmuir-Blodgett to Self-Assembly*, Academic Press Inc., San Diego, CA, USA **1991**.
- [15] M. Mastrangeli, S. Abbasi, C. Varel, C. Van Hoof, J.-P. Celis, K. F. Böhringer, *J. Micromech. Microeng.* **2009**, *19*, 83001.
- [16] K. J. M. Bishop, C. E. Wilmer, S. Soh, B. A. Grzybowski, *Small* **2009**, *5*, 1600.
- [17] S. Brittain, K. Paul, X.-M. Zhao, G. Whitesides, *Phys. World* **1998**, *11*, 31.
- [18] M. J. Madou, *Fundamentals of Microfabrication and Nanotechnology, Three-Volume Set*, 3rd ed., CRC Press, Boca Raton, FL, USA **2011**.
- [19] M. Piel, M. Théry, *Micropatterning in Cell Biology*, Academic Press, Waltham, MA, USA **2014**.
- [20] P. Bajaj, R. M. Schweller, A. Khademhosseini, J. L. West, R. Bashir, *Annu. Rev. Biomed. Eng.* **2014**, *16*, 247.
- [21] L. G. Zhang, J. P. Fisher, K. Leong, *3D Bioprinting and Nanotechnology in Tissue Engineering and Regenerative Medicine*, Academic Press, Waltham, MA, USA **2015**.
- [22] F. P. W. Melchels, J. Feijen, D. W. Grijpma, *Biomaterials* **2010**, *31*, 6121.
- [23] S. V. Murphy, A. Atala, *Nat. Biotechnol.* **2014**, *32*, 773.
- [24] W. Oropallo, L. A. Piegl, *Eng. Comput.* **2015**, *32*, 135.
- [25] W. Zhu, X. Ma, M. Gou, D. Mei, K. Zhang, S. Chen, *Curr. Opin. Biotechnol.* **2016**, *40*, 103.
- [26] S. Reyntjens, R. Puers, J. Micromech. *Microeng.* **2001**, *11*, 287.
- [27] S. H. Gellman, *Acc. Chem. Res.* **1998**, *31*, 173.
- [28] D. J. Hill, M. J. Mio, R. B. Prince, T. S. Hughes, J. S. Moore, *Chem. Rev.* **2001**, *101*, 3893.
- [29] G. Guichard, I. Huc, *Chem. Commun.* **2011**, *47*, 5933.
- [30] F. Zhang, J. Nangreave, Y. Liu, H. Yan, *J. Am. Chem. Soc.* **2014**, *136*, 11198.
- [31] P. Wang, T. A. Meyer, V. Pan, P. K. Dutta, Y. Ke, *Chem* **2017**, *2*, 359.
- [32] E. G. Baker, G. J. Bartlett, K. L. Porter Goff, D. N. Woolfson, *Acc. Chem. Res.* **2017**, *50*, 2085.
- [33] N. C. Seeman, H. F. Sleiman, *Nat. Rev. Mater.* **2017**, *3*, 17068.
- [34] F. Hong, F. Zhang, Y. Liu, H. Yan, *Chem. Rev.* **2017**, *117*, 12584.
- [35] R. R. A. Syms, E. M. Yeatman, V. M. Bright, G. M. Whitesides, *J. Microelectromech. Syst.* **2003**, *12*, 387.
- [36] C. L. Randall, T. G. Leong, N. Bassik, D. H. Gracias, *Adv. Drug Delivery Rev.* **2007**, *59*, 1547.
- [37] Y. Mei, G. Huang, A. A. Solovev, E. B. Ureña, I. Mönch, F. Ding, T. Reindl, R. K. Y. Fu, P. K. Chu, O. G. Schmidt, *Adv. Mater.* **2008**, *20*, 4085.
- [38] R. Fernandes, D. H. Gracias, *Mater. Today* **2009**, *12*, 14.
- [39] T. G. Leong, A. M. Zarafshar, D. H. Gracias, *Small* **2010**, *6*, 792.
- [40] Y. Mei, A. A. Solovev, S. Sanchez, O. G. Schmidt, *Chem. Soc. Rev.* **2011**, *40*, 2109.
- [41] J. S. Randhawa, K. E. Laflin, N. Seelam, D. H. Gracias, *Adv. Funct. Mater.* **2011**, *21*, 2395.
- [42] L. Ionov, *Soft Matter* **2011**, *7*, 6786.
- [43] J. A. Rogers, M. G. Lagally, R. G. Nuzzo, *Nature* **2011**, *477*, 45.
- [44] C. L. Randall, E. Gultepe, D. H. Gracias, *Trends Biotechnol.* **2012**, *30*, 138.
- [45] L. Ionov, *Macromol. Chem. Phys.* **2012**, *214*, 1178.
- [46] L. Ionov, *Polym. Rev.* **2013**, *53*, 92.
- [47] D. H. Gracias, *Curr. Opin. Chem. Eng.* **2013**, *2*, 112.
- [48] E. A. Peraza-Hernandez, D. J. Hartl, R. J. Malak Jr., D. C. Lagoudas, *Smart Mater. Struct.* **2014**, *23*, 094001.
- [49] J. Rogers, Y. Huang, O. G. Schmidt, D. H. Gracias, *MRS Bull.* **2016**, *41*, 123.
- [50] Y. Liu, J. Genzer, M. D. Dickey, *Prog. Polym. Sci.* **2016**, *52*, 79.
- [51] Y. Zhang, F. Zhang, Z. Yan, Q. Ma, X. Li, Y. Huang, J. A. Rogers, *Nat. Rev. Mater.* **2017**, *2*, 17019.
- [52] S.-J. Jeon, A. W. Hauser, R. C. Hayward, *Acc. Chem. Res.* **2017**, *50*, 161.
- [53] A. Kirillova, R. Maxson, G. Stoychev, C. T. Gomillion, L. Ionov, *Adv. Mater.* **2017**, *29*, 1703443.
- [54] M. Johnson, Y. Chen, S. Hovet, S. Xu, B. Wood, H. Ren, J. Tokuda, Z. T. H. Tse, *Int. J. Comput. Assist. Radiol. Surg.* **2017**, *12*, 2023.
- [55] S. Böttner, M. R. Jorgensen, O. G. Schmidt, *Scripta Mater.* **2016**, *122*, 119.
- [56] D. Rus, M. T. Tolley, *Nat. Rev. Mater.* **2018**, *3*, 101.
- [57] K. A. Dill, *Biochemistry* **1990**, *29*, 7133.
- [58] R. Keller, D. Shook, *BMC Biol.* **2011**, *9*, 90.

- [59] A. E. Shyer, T. Tallinen, N. L. Nerurkar, Z. Wei, E. S. Gil, D. L. Kaplan, C. J. Tabin, L. Mahadevan, *Science* **2013**, 342, 212.
- [60] M. Misra, B. Audoly, S. Y. Shvartsman, *Philos. Trans. R. Soc. Lond. B Biol. Sci.* **2017**, 372, 20150515.
- [61] D. Fristrom, *Tissue Cell* **1988**, 20, 645.
- [62] L. A. Taber, *Appl. Mech. Rev.* **1995**, 48, 487.
- [63] F. Haas, S. Gorb, R. Blickhan, *Proc. R. Soc. Lond. B* **2000**, 267, 1375.
- [64] K. Saito, S. Nomura, S. Yamamoto, R. Niiyama, Y. Okabe, *Proc. Natl. Acad. Sci. USA* **2017**, 114, 5624.
- [65] J. N. Israelachvili, *Intermolecular and Surface Forces (3rd edition)*, Academic Press, San Diego, CA, USA **2011**.
- [66] W. Xu, K. S. Kwok, D. H. Gracias, *Acc. Chem. Res.* **2018**, 51, 436.
- [67] V. B. Shenoy, D. H. Gracias, *MRS Bull.* **2012**, 37, 847.
- [68] J.-H. Cho, D. H. Gracias, *Nano Lett.* **2009**, 9, 4049.
- [69] H. R. Kwag, J.-H. Cho, S.-Y. Park, J. Park, D. H. Gracias, *Faraday Discuss.* **2016**, 191, 61.
- [70] S. Tibbitts, *Archit. Design* **2014**, 84, 116.
- [71] A. Sydney Gladman, E. A. Matsumoto, R. G. Nuzzo, L. Mahadevan, J. A. Lewis, *Nat. Mater.* **2016**, 15, 413.
- [72] Y.-C. Li, Y. S. Zhang, A. Akpek, S. R. Shin, A. Khademhosseini, *Biofabrication* **2016**, 9, 012001.
- [73] L. Ionov, *Adv. Healthcare Mater.* **2018**, 1800412.
- [74] M. Jamal, A. M. Zarafshar, D. H. Gracias, *Nat. Commun.* **2011**, 2, 527.
- [75] L. G. Griffith, G. Naughton, *Science* **2002**, 295, 1009.
- [76] A. Atala, F. K. Kasper, A. G. Mikos, *Sci. Transl. Med.* **2012**, 4, 160rv12.
- [77] W. Xu, Z. Qin, C.-T. Chen, H. R. Kwag, Q. Ma, A. Sarkar, M. J. Buehler, D. H. Gracias, *Sci. Adv.* **2017**, 3, e1701084.
- [78] M. Z. Miskin, K. J. Dorsey, B. Bircan, Y. Han, D. A. Muller, P. L. McEuen, I. Cohen, *Proc. Natl. Acad. Sci. USA* **2018**, 115, 466.
- [79] C. M. Dobson, *Nature* **2003**, 426, 884.
- [80] P. J. Thomas, B. H. Qu, P. L. Pedersen, *Trends Biochem. Sci.* **1995**, 20, 456.
- [81] D. J. Selkoe, *Nature* **2003**, 426, 900.
- [82] F. U. Hartl, A. Bracher, M. Hayer-Hartl, *Nature* **2011**, 475, 324.
- [83] J. Widom, *Annu. Rev. Biophys. Biophys. Chem.* **1989**, 18, 365.
- [84] R. Everaers, H. Schiessel, *J. Phys.: Condens. Matter* **2015**, 27, 060301.
- [85] J.-L. Schmitt, A.-M. Stadler, N. Kyritsakas, J.-M. Lehn, *Helv. Chim. Acta* **2003**, 86, 1598.
- [86] M. Hagihara, N. J. Anthony, T. J. Stout, J. Clardy, S. L. Schreiber, *J. Am. Chem. Soc.* **1992**, 114, 6568.
- [87] R. Scott Lokey, B. L. Iverson, *Nature* **1995**, 375, 303.
- [88] M. Gude, U. Piarelli, D. Potenza, B. Salom, C. Gennari, *Tetrahedron Lett.* **1996**, 37, 8589.
- [89] N. C. Seeman, *J. Theor. Biol.* **1982**, 99, 237.
- [90] N. C. Seeman, *Annu. Rev. Biophys. Biomol. Struct.* **1998**, 27, 225.
- [91] E. Wfree, F. Liu, L. A. Wenzler, N. C. Seeman, *Nature* **1998**, 394, 539.
- [92] P. W. K. Rothmund, *Nature* **2006**, 440, 297.
- [93] B. Wei, M. Dai, P. Yin, *Nature* **2012**, 485, 623.
- [94] D. Han, X. Qi, C. Myhrvold, B. Wang, M. Dai, S. Jiang, M. Bates, Y. Liu, B. An, F. Zhang, H. Yan, P. Yin, *Science* **2017**, 358, eaao2648.
- [95] R. Carlson, *Nat. Biotechnol.* **2009**, 27, 1091.
- [96] J. Chao, D. Zhu, Y. Zhang, L. Wang, C. Fan, *Biosens. Bioelectron.* **2016**, 76, 68.
- [97] Y. Flores Bueso, M. Tangney, *Trends Biotechnol.* **2017**, 35, 373.
- [98] Y. Ke, S. Lindsay, Y. Chang, Y. Liu, H. Yan, *Science* **2008**, 319, 180.
- [99] C. Teller, I. Willner, *Curr. Opin. Biotechnol.* **2010**, 21, 376.
- [100] A. Kuzuya, Y. Sakai, T. Yamazaki, Y. Xu, M. Komiyama, *Nat. Commun.* **2011**, 2, 449.
- [101] F. Wang, X. Liu, I. Willner, *Angew. Chem. Int. Ed. Engl.* **2015**, 54, 1098.
- [102] H. A. Becerril, A. T. Woolley, *Chem. Soc. Rev.* **2009**, 38, 329.
- [103] S. Pal, Z. Deng, B. Ding, H. Yan, Y. Liu, *Angew. Chem., Int. Ed. Engl.* **2010**, 49, 2700.
- [104] A. Samanta, I. L. Medintz, *Nanoscale* **2016**, 8, 9037.
- [105] Z. Chen, C. Liu, F. Cao, J. Ren, X. Qu, *Chem. Soc. Rev.* **2018**, 47, 4017.
- [106] H. Kim, S. P. Surwade, A. Powell, C. O'Donnell, H. Liu, *Chem. Mater.* **2014**, 26, 5265.
- [107] S. Ramakrishnan, G. Krainer, G. Grundmeier, M. Schlierf, A. Keller, *Nanoscale* **2016**, 8, 10398.
- [108] B. R. Eggins, *Chemical Sensors and Biosensors*, John Wiley & Sons, West Sussex, UK **2002**.
- [109] A. Weltin, J. Kieninger, G. A. Urban, *Anal. Bioanal. Chem.* **2016**, 408, 4503.
- [110] T. Xiao, F. Wu, J. Hao, M. Zhang, P. Yu, L. Mao, *Anal. Chem.* **2017**, 89, 300.
- [111] A.-M. Pappa, O. Parlak, G. Scheiblin, P. Mailley, A. Salleo, R. M. Owens, *Trends Biotechnol.* **2018**, 36, 45.
- [112] R. Lind, P. Connolly, C. D. W. Wilkinson, R. D. Thomson, *Sens. Actuators, B* **1991**, 3, 23.
- [113] C. S. Bausch, C. Heyn, W. Hansen, I. M. A. Wolf, B.-P. Diercks, A. H. Guse, R. H. Blick, *Sci. Rep.* **2017**, 7, 41584.
- [114] Q. Jin, M. Li, B. Polat, S. K. Paidi, A. Dai, A. Zhang, J. V. Pagaduan, I. Barman, D. H. Gracias, *Angew. Chem., Int. Ed. Engl.* **2017**, 56, 3822.
- [115] J. Cools, Q. Jin, E. Yoon, D. Alba Burbano, Z. Luo, D. Cuypers, G. Callewaert, D. Braeken, D. H. Gracias, *Adv. Sci.* **2018**, 5, 1700731.
- [116] S. M. Weiz, M. Medina-Sánchez, O. G. Schmidt, *Adv. Biosyst.* **2018**, 2, 1700193.
- [117] N. A. W. Bell, U. F. Keyser, *FEBS Lett.* **2014**, 588, 3564.
- [118] A. Shaw, V. Lundin, E. Petrova, F. Fördös, E. Benson, A. Al-Amin, A. Herland, A. Blokzijl, B. Högberg, A. I. Teixeira, *Nat. Methods* **2014**, 11, 841.
- [119] C. E. Castro, H. Dietz, B. Högberg, *MRS Bull.* **2017**, 42, 925.
- [120] S. M. Harazim, V. A. Bolaños Quiñones, S. Kiravittaya, S. Sanchez, O. G. Schmidt, *Lab Chip* **2012**, 12, 2649.
- [121] S. M. Woo, C. M. Gabardo, L. Soleymani, *Anal. Chem.* **2014**, 86, 12341.
- [122] Z. Yan, M. Han, Y. Shi, A. Badea, Y. Yang, A. Kulkarni, E. Hanson, M. E. Kandel, X. Wen, F. Zhang, Y. Luo, Q. Lin, H. Zhang, X. Guo, Y. Huang, K. Nan, S. Jia, A. W. Oraharn, M. B. Mevis, J. Lim, X. Guo, M. Gao, W. Ryu, K. J. Yu, B. G. Nicolau, A. Petronico, S. S. Rubakhin, J. Lou, P. M. Ajayan, K. Thornton, G. Popescu, D. Fang, J. V. Sweedler, P. V. Braun, H. Zhang, R. G. Nuzzo, Y. Huang, Y. Zhang, J. A. Rogers, *Proc. Natl. Acad. Sci. USA* **2017**, 114, E9455.
- [123] M. Pilo-Pais, A. Watson, S. Demers, T. H. LaBean, G. Finkelstein, *Nano Lett.* **2014**, 14, 2099.
- [124] V. V. Thacker, L. O. Herrmann, D. O. Sigle, T. Zhang, T. Liedl, J. J. Baumberg, U. F. Keyser, *Nat. Commun.* **2014**, 5, 3448.
- [125] P. Zhan, T. Wen, Z.-G. Wang, Y. He, J. Shi, T. Wang, X. Liu, G. Lu, B. Ding, *Angew. Chem., Int. Ed. Engl.* **2018**, 57, 2846.
- [126] A. Puchkova, C. Vietz, E. Pibiri, B. Wünsch, M. Sanz Paz, G. P. Acuna, P. Tinnefeld, *Nano Lett.* **2015**, 15, 8354.
- [127] I. H. Stein, V. Schüller, P. Böhm, P. Tinnefeld, T. Liedl, *ChemPhysChem* **2011**, 12, 689.
- [128] C. Steinhauer, R. Jungmann, T. Sobey, F. Simmel, P. Tinnefeld, *Angew. Chem., Int. Ed.* **2009**, 48, 8870.
- [129] J.-H. Cho, M. D. Keung, N. Verellen, L. Lagae, V. V. Moshchalkov, P. Van Dorpe, D. H. Gracias, *Small* **2011**, 7, 1943.
- [130] V. V. R. Sai, T. Kundu, S. Mukherji, *Biosens. Bioelectron.* **2009**, 24, 2804.
- [131] G. Liang, Z. Zhao, Y. Wei, K. Liu, W. Hou, Y. Duan, *RSC Adv.* **2015**, 5, 23990.
- [132] A. da S. Arcas, F. da S. Dutra, R. C. S. B. Allil, M. M. Werneck, *Sensors* **2018**, 18, 648.

- [133] V. Y. Prinz, V. A. Seleznev, A. K. Gutakovskiy, A. V. Chehovskiy, V. V. Preobrazhenskii, M. A. Putyato, T. A. Gavrilova, *Physica E* **2000**, 6, 828.
- [134] O. G. Schmidt, K. Eberl, *Nature* **2001**, 410, 168.
- [135] Q. Guo, Z. Di, M. G. Lagally, Y. Mei, *Mater. Sci. Eng., R* **2018**, 128, 1.
- [136] K. J. Vahala, *Nature* **2003**, 424, 839.
- [137] E. J. Smith, S. Schulze, S. Kiravittaya, Y. Mei, S. Sanchez, O. G. Schmidt, *Nano Lett.* **2011**, 11, 4037.
- [138] L. Ma, S. Li, V. A. Bolaños Quiñones, L. Yang, W. Xi, M. Jorgensen, S. Baunack, Y. Mei, S. Kiravittaya, O. G. Schmidt, *Adv. Mater.* **2013**, 25, 2357.
- [139] M.-C. Chuang, Y.-L. Yang, T.-F. Tseng, T. Chou, S.-L. Lou, J. Wang, *Talanta* **2010**, 81, 15.
- [140] B. Tian, T. Cohen-Karni, Q. Qing, X. Duan, P. Xie, C. M. Lieber, *Science* **2010**, 329, 830.
- [141] C. S. Martinez-Cisneros, S. Sanchez, W. Xi, O. G. Schmidt, *Nano Lett.* **2014**, 14, 2219.
- [142] M. Medina-Sánchez, B. Ibarlucea, N. Pérez, D. D. Karnaushenko, S. M. Weiz, L. Baraban, G. Cuniberti, O. G. Schmidt, *Nano Lett.* **2016**, 16, 4288.
- [143] T.-R. Ger, H.-T. Huang, C.-Y. Huang, M.-F. Lai, *Lab Chip* **2013**, 13, 4225.
- [144] I. Mönch, D. Makarov, R. Koseva, L. Baraban, D. Karnaushenko, C. Kaiser, K.-F. Arndt, O. G. Schmidt, *ACS Nano* **2011**, 5, 7436.
- [145] D. D. Karnaushenko, D. Karnaushenko, D. Makarov, O. G. Schmidt, *NPG Asia Mater.* **2015**, 7, e188.
- [146] D. Karnaushenko, N. Münzenrieder, D. D. Karnaushenko, B. Koch, A. K. Meyer, S. Baunack, L. Petti, G. Tröster, D. Makarov, O. G. Schmidt, *Adv. Mater.* **2015**, 27, 6797.
- [147] Y. Yin, Y. Chen, E. S. G. Naz, X. Lu, S. Li, V. Engemaier, L. Ma, O. G. Schmidt, *ACS Photonics* **2017**, 4, 736.
- [148] G. Huang, Y. Mei, *Small* **2018**, 14, 1703665.
- [149] E. J. Smith, W. Xi, D. Makarov, I. Mönch, S. Harazim, V. A. Bolaños Quiñones, C. K. Schmidt, Y. Mei, S. Sanchez, O. G. Schmidt, *Lab Chip* **2012**, 12, 1917.
- [150] T. Deng, C. Yoon, Q. Jin, M. Li, Z. Liu, D. H. Gracias, *Appl. Phys. Lett.* **2015**, 106, 203108.
- [151] J. Liu, C. Xie, X. Dai, L. Jin, W. Zhou, C. M. Lieber, *Proc. Natl. Acad. Sci. USA* **2013**, 110, 6694.
- [152] X. Dai, G. Hong, T. Gao, C. M. Lieber, *Acc. Chem. Res.* **2018**, 51, 309.
- [153] K. Malachowski, M. Jamal, Q. Jin, B. Polat, C. J. Morris, D. H. Gracias, *Nano Lett.* **2014**, 14, 4164.
- [154] C.-C. Fu, A. Grimes, M. Long, C. G. L. Ferri, B. D. Rich, S. Ghosh, S. Ghosh, L. P. Lee, A. Gopinathan, M. Khine, *Adv. Mater.* **2009**, 21, 4472.
- [155] R. C. Adams-McGavin, Y. Chan, C. M. Gabardo, J. Yang, M. Skreta, B. C. Fung, L. Soleymani, *Electrochim. Acta* **2017**, 242, 1.
- [156] C. M. Gabardo, A. Hosseini, L. Soleymani, *IEEE Nanotechnol. Mag.* **2016**, 10, 6.
- [157] Y. Sun, W. M. Choi, H. Jiang, Y. Y. Huang, J. A. Rogers, *Nat. Nanotechnol.* **2006**, 1, 201.
- [158] S. Xu, Z. Yan, K.-I. Jang, W. Huang, H. Fu, J. Kim, Z. Wei, M. Flavin, J. McCracken, R. Wang, A. Badea, Y. Liu, D. Xiao, G. Zhou, J. Lee, H. U. Chung, H. Cheng, W. Ren, A. Banks, X. Li, U. Paik, R. G. Nuzzo, Y. Huang, Y. Zhang, J. A. Rogers, *Science* **2015**, 347, 154.
- [159] Z. Yan, F. Zhang, J. Wang, F. Liu, X. Guo, K. Nan, Q. Lin, M. Gao, D. Xiao, Y. Shi, Y. Qiu, H. Luan, J. H. Kim, Y. Wang, H. Luo, M. Han, Y. Huang, Y. Zhang, J. A. Rogers, *Adv. Funct. Mater.* **2016**, 26, 2629.
- [160] H. Fu, K. Nan, W. Bai, W. Huang, K. Bai, L. Lu, C. Zhou, Y. Liu, F. Liu, J. Wang, M. Han, Z. Yan, H. Luan, Y. Zhang, Y. Zhang, J. Zhao, X. Cheng, M. Li, J. W. Lee, Y. Liu, D. Fang, X. Li, Y. Huang, Y. Zhang, J. A. Rogers, *Nat. Mater.* **2018**, 17, 268.
- [161] G. M. Whitesides, *Nature* **2006**, 442, 368.
- [162] A. Khademhosseini, R. Langer, J. Borenstein, J. P. Vacanti, *Proc. Natl. Acad. Sci. USA* **2006**, 103, 2480.
- [163] J. Melin, S. R. Quake, *Annu. Rev. Biophys. Biomol. Struct.* **2007**, 36, 213.
- [164] D. Psaltis, S. R. Quake, C. Yang, *Nature* **2006**, 442, 381.
- [165] P. Abgrall, A.-M. Gué, *J. Micromech. Microeng.* **2007**, 17, R15.
- [166] A. Bein, W. Shin, S. Jalili-Firoozinezhad, M. H. Park, A. Sontheimer-Phelps, A. Tovaglieri, A. Chalkiadaki, H. J. Kim, D. E. Ingber, *Cell. Mol. Gastroenterol. Hepatol.* **2018**, 5, 659.
- [167] C. M. B. Ho, S. H. Ng, K. H. H. Li, Y.-J. Yoon, *Lab Chip* **2015**, 15, 3627.
- [168] R. D. Sochol, E. Sweet, C. C. Glick, S.-Y. Wu, C. Yang, M. Restaino, L. Lin, *Microelectron. Eng.* **2018**, 189, 52.
- [169] A. W. Martinez, S. T. Phillips, G. M. Whitesides, *Proc. Natl. Acad. Sci. USA* **2008**, 105, 19606.
- [170] Y. Xia, J. Si, Z. Li, *Biosens. Bioelectron.* **2016**, 77, 774.
- [171] H. Liu, R. M. Crooks, *J. Am. Chem. Soc.* **2011**, 133, 17564.
- [172] L. Ge, S. Wang, X. Song, S. Ge, J. Yu, *Lab Chip* **2012**, 12, 3150.
- [173] A. V. Govindarajan, S. Ramachandran, G. D. Vigil, P. Yager, K. F. Böhringer, *Lab Chip* **2012**, 12, 174.
- [174] S. Wang, W. Dai, L. Ge, M. Yan, J. Yu, X. Song, S. Ge, J. Huang, *Chem. Commun.* **2012**, 48, 9971.
- [175] S. Wang, L. Ge, M. Yan, J. Yu, X. Song, S. Ge, J. Huang, *Sens. Actuators, B* **2013**, 176, 1.
- [176] X. Zhang, J. Li, C. Chen, B. Lou, L. Zhang, E. Wang, *Chem. Commun.* **2013**, 49, 3866.
- [177] B. Kalish, H. Tsutsui, *Lab Chip* **2014**, 14, 4354.
- [178] S. Choi, S.-K. Kim, G.-J. Lee, H.-K. Park, *Sens. Actuators, B* **2015**, 219, 245.
- [179] L. Wu, C. Ma, L. Ge, Q. Kong, M. Yan, S. Ge, J. Yu, *Biosens. Bioelectron.* **2015**, 63, 450.
- [180] X. Li, X. Liu, *Adv. Healthcare Mater.* **2016**, 5, 1326.
- [181] J. Ding, B. Li, L. Chen, W. Qin, *Angew. Chem., Int. Ed. Engl.* **2016**, 55, 13033.
- [182] W. Li, D. Qian, Q. Wang, Y. Li, N. Bao, H. Gu, C. Yu, *Sens. Actuators, B* **2016**, 231, 230.
- [183] C.-C. Wang, J. W. Hennek, A. Ainla, A. A. Kumar, W.-J. Lan, J. Im, B. S. Smith, M. Zhao, G. M. Whitesides, *Anal. Chem.* **2016**, 88, 6326.
- [184] B. Li, Z. Zhang, J. Qi, N. Zhou, S. Qin, J. Choo, L. Chen, *ACS Sens.* **2017**, 2, 243.
- [185] Z. Yang, G. Xu, J. Reboud, S. A. Ali, G. Kaur, J. McGiven, N. Boby, P. K. Gupta, P. Chaudhuri, J. M. Cooper, *ACS Sens.* **2018**, 3, 403.
- [186] Z.-X. Lao, Y.-L. Hu, D. Pan, R.-Y. Wang, C.-C. Zhang, J.-C. Ni, B. Xu, J.-W. Li, D. Wu, J.-R. Chu, *Small* **2017**, 13, 1603957.
- [187] A. Malachias, Y. Mei, R. K. Annabattula, C. Deneke, P. R. Onck, O. G. Schmidt, *ACS Nano* **2008**, 2, 1715.
- [188] Y. Mei, S. Kiravittaya, S. Harazim, O. G. Schmidt, *Mater. Sci. Eng., R* **2010**, 70, 209.
- [189] C. M. Gabardo, R. C. Adams-McGavin, O. M. Vanderfleet, L. Soleymani, *Analyst* **2015**, 140, 5781.
- [190] J. Sun, Y. Xianyu, M. Li, W. Liu, L. Zhang, D. Liu, C. Liu, G. Hu, X. Jiang, *Nanoscale* **2013**, 5, 5262.
- [191] L. Mahadevan, S. Rica, *Science* **2005**, 307, 1740.
- [192] U. N. Hiller, in *Functional Surfaces in Biology: Little Structures with Big Effects*, (Ed: S. N. Gorb), Vol. 1, Springer Science+Business Media, Inc., New York, NY, USA **2009**, p. 47.
- [193] G. S. Watson, D. W. Green, L. Schwarzkopf, X. Li, B. W. Cribb, S. Myhra, J. A. Watson, *Acta Biomater.* **2015**, 21, 109.
- [194] G. Cammarota, A. Martino, G. A. Pirozzi, R. Cianci, F. Cremonini, G. Zuccalà, L. Cuoco, V. Ojetti, M. Montalto, F. M. Vecchio, A. Gasbarrini, G. Gasbarrini, *Gastrointest. Endosc.* **2004**, 60, 732.
- [195] B. Draganski, C. Gaser, V. Busch, G. Schuierer, U. Bogdahn, A. May, *Nature* **2004**, 427, 311.

- [196] C. D. Good, I. S. Johnsrude, J. Ashburner, R. N. Henson, K. J. Friston, R. S. J. Frackowiak, *Neuroimage* **2001**, 14, 21.
- [197] J. Morys, O. Narkiewicz, H. M. Wisniewski, *Brain Res.* **1993**, 616, 176.
- [198] M. Kumar, R. Gupta, B. Kaul, Y. Agarwal, *Astrocyte* **2016**, 2, 209.
- [199] J. R. Daube, S. M. Chou, *Neurology* **1966**, 16, 179.
- [200] J. C. Hayward, D. S. Titelbaum, R. R. Clancy, R. A. Zimmerman, *J. Child Neurol.* **1991**, 6, 109.
- [201] S. D. Joshi, L. A. Davidson, *Biomech. Model. Mechanobiol.* **2012**, 11, 1109.
- [202] J. B. Bard, A. S. Ross, *Dev. Biol.* **1982**, 92, 87.
- [203] U. Cheema, R. A. Brown, B. Alp, A. J. MacRobert, *Cell. Mol. Life Sci.* **2008**, 65, 177.
- [204] J. L. Horning, S. K. Sahoo, S. Vijayaraghavalu, S. Dimitrijevic, J. K. Vasir, T. K. Jain, A. K. Panda, V. Labhasetwar, *Mol. Pharm.* **2008**, 5, 849.
- [205] C. Fischbach, H. J. Kong, S. X. Hsiong, M. B. Evangelista, W. Yuen, D. J. Mooney, *Proc. Natl. Acad. Sci. USA* **2009**, 106, 399.
- [206] D. Yamazaki, S. Kurisu, T. Takenawa, *Oncogene* **2009**, 28, 1570.
- [207] B. Weigelt, C. M. Ghajar, M. J. Bissell, *Adv. Drug Delivery Rev.* **2014**, 69, 42.
- [208] V. van Duinen, S. J. Trietsch, J. Joore, P. Vulto, T. Hankemeier, *Curr. Opin. Biotechnol.* **2015**, 35, 118.
- [209] M. Simian, M. J. Bissell, *J. Cell Biol.* **2017**, 216, 31.
- [210] A. Görlach, P. Herter, H. Hentschel, P. J. Frosch, H. Acker, *Int. J. Cancer* **1994**, 56, 249.
- [211] P. Zhuang, A. X. Sun, J. An, C. K. Chua, S. Y. Chew, *Biomaterials* **2018**, 154, 113.
- [212] W. Xi, C. K. Schmidt, S. Sanchez, D. H. Gracias, R. E. Carazo-Salas, S. P. Jackson, O. G. Schmidt, *Nano Lett.* **2014**, 14, 4197.
- [213] W. Xi, C. K. Schmidt, S. Sanchez, D. H. Gracias, R. E. Carazo-Salas, R. Butler, N. Lawrence, S. P. Jackson, O. G. Schmidt, *ACS Nano* **2016**, 10, 5835.
- [214] D. J. Beebe, G. A. Mensing, G. M. Walker, *Annu. Rev. Biomed. Eng.* **2002**, 4, 261.
- [215] S. K. Sia, G. M. Whitesides, *Electrophoresis* **2003**, 24, 3563.
- [216] L. K. Fiddes, N. Raz, S. Srigunapalan, E. Tumarkan, C. A. Simmons, A. R. Wheeler, E. Kumacheva, *Biomaterials* **2010**, 31, 3459.
- [217] G. Stoychev, N. Pureskiy, L. Ionov, *Soft Matter* **2011**, 7, 3277.
- [218] S. Pedron, S. van Lierop, P. Horstman, R. Penterman, D. J. Broer, E. Peeters, *Adv. Funct. Mater.* **2011**, 21, 1624.
- [219] M. Eiraku, N. Takata, H. Ishibashi, M. Kawada, E. Sakakura, S. Okuda, K. Sekiguchi, T. Adachi, Y. Sasai, *Nature* **2011**, 472, 51.
- [220] M. Takasato, P. X. Er, M. Becroft, J. M. Vanslambrouck, E. G. Stanley, A. G. Elefanti, M. H. Little, *Nat. Cell Biol.* **2014**, 16, 118.
- [221] D. Pamies, P. Barreras, K. Block, G. Makri, A. Kumar, D. Wiersma, L. Smirnova, C. Zang, J. Bressler, K. M. Christian, G. Harris, G.-L. Ming, C. J. Berlinicke, K. Kyro, H. Song, C. A. Pardo, T. Hartung, H. T. Hogberg, *ALTEX* **2017**, 34, 362.
- [222] X. Yin, B. E. Mead, H. Safaei, R. Langer, J. M. Karp, O. Levy, *Cell Stem Cell* **2016**, 18, 25.
- [223] H. Shirai, M. Mandai, K. Matsushita, A. Kuwahara, S. Yonemura, T. Nakano, J. Assawachananont, T. Kimura, K. Saito, H. Terasaki, M. Eiraku, Y. Sasai, M. Takahashi, *Proc. Natl. Acad. Sci. USA* **2016**, 113, E81.
- [224] G. Huang, Y. Mei, D. J. Thurmer, E. Coric, O. G. Schmidt, *Lab Chip* **2009**, 9, 263.
- [225] S. Schulze, G. Huang, M. Krause, D. Aubyn, V. A. Bolaños Quiñones, C. K. Schmidt, Y. Mei, O. G. Schmidt, *Adv. Eng. Mater.* **2010**, 12, B558.
- [226] M. Jamal, N. Bassik, J.-H. Cho, C. L. Randall, D. H. Gracias, *Biomaterials* **2010**, 31, 1683.
- [227] S. Zakharchenko, E. Sperling, L. Ionov, *Biomacromolecules* **2011**, 12, 2211.
- [228] B. Yuan, Y. Jin, Y. Sun, D. Wang, J. Sun, Z. Wang, W. Zhang, X. Jiang, *Adv. Mater.* **2012**, 24, 890.
- [229] P. Gong, W. Zheng, Z. Huang, W. Zhang, D. Xiao, X. Jiang, *Adv. Funct. Mater.* **2013**, 23, 42.
- [230] M. Jamal, S. S. Kadam, R. Xiao, F. Jivan, T.-M. Onn, R. Fernandes, T. D. Nguyen, D. H. Gracias, *Adv. Healthcare Mater.* **2013**, 2, 1142.
- [231] H. R. Kwag, J. V. Serbo, P. Korangath, S. Sukumar, L. H. Romer, D. H. Gracias, *Tissue Eng. Part C Methods* **2016**, 22, 398.
- [232] J. Sang, X. Li, Y. Shao, Z. Li, J. Fu, *ACS Biomater. Sci. Eng.* **2017**, 3, 2860.
- [233] T. F. Teshima, H. Nakashima, Y. Ueno, S. Sasaki, C. S. Henderson, S. Tsukada, *Sci. Rep.* **2017**, 7, 17376.
- [234] V. Stroganov, J. Pant, G. Stoychev, A. Janke, D. Jehnichen, A. Fery, H. Handa, L. Ionov, *Adv. Funct. Mater.* **2018**, 28, 1706248.
- [235] Q. He, T. Okajima, H. Onoe, A. Subagyo, K. Sueoka, K. Kuribayashi-Shigetomi, *Sci. Rep.* **2018**, 8, 4556.
- [236] R. Arayanarakool, A. K. Meyer, L. Helbig, S. Sanchez, O. G. Schmidt, *Lab Chip* **2015**, 15, 2981.
- [237] S. Cheng, Y. Jin, N. Wang, F. Cao, W. Zhang, W. Bai, W. Zheng, X. Jiang, *Adv. Mater.* **2017**, 29, 1700171.
- [238] Y. Li, K. Jiang, J. Feng, J. Liu, R. Huang, Z. Chen, J. Yang, Z. Dai, Y. Chen, N. Wang, W. Zhang, W. Zheng, G. Yang, X. Jiang, *Adv. Healthcare Mater.* **2017**, 6, 1601343.
- [239] K. Kuribayashi-Shigetomi, H. Onoe, S. Takeuchi, *PLoS One* **2012**, 7, e51085.
- [240] V. P. Torchilin, *Nat. Rev. Drug Discovery* **2014**, 13, 813.
- [241] A. Kakkar, G. Traverso, O. C. Farokhzad, R. Weissleder, R. Langer, *Nat. Rev. Chem.* **2017**, 1, 0063.
- [242] Q. Jiang, C. Song, J. Nangreave, X. Liu, L. Lin, D. Qiu, Z.-G. Wang, G. Zou, X. Liang, H. Yan, B. Ding, *J. Am. Chem. Soc.* **2012**, 134, 13396.
- [243] Q. Zhang, Q. Jiang, N. Li, L. Dai, Q. Liu, L. Song, J. Wang, Y. Li, J. Tian, B. Ding, Y. Du, *ACS Nano* **2014**, 8, 6633.
- [244] H. Lee, A. K. R. Lytton-Jean, Y. Chen, K. T. Love, A. I. Park, E. D. Karagiannis, A. Sehgal, W. Querbes, C. S. Zurenko, M. Jayaraman, C. G. Peng, K. Charisse, A. Borodovsky, M. Manoharan, J. S. Donahoe, J. Truelove, M. Nahrenndorf, R. Langer, D. G. Anderson, *Nat. Nanotechnol.* **2012**, 7, 389.
- [245] A. Azam, K. E. Laffin, M. Jamal, R. Fernandes, D. H. Gracias, *Biomed. Microdevices* **2011**, 13, 51.
- [246] T. G. Leong, B. R. Benson, E. K. Call, D. H. Gracias, *Small* **2008**, 4, 1605.
- [247] S. Zakharchenko, N. Pureskiy, G. Stoychev, M. Stamm, L. Ionov, *Soft Matter* **2010**, 6, 2633.
- [248] J. Guan, H. He, L. J. Lee, D. J. Hansford, *Small* **2007**, 3, 412.
- [249] R. Fernandes, D. H. Gracias, *Adv. Drug Delivery Rev.* **2012**, 64, 1579.
- [250] T. S. Shim, S.-H. Kim, C.-J. Heo, H. C. Jeon, S.-M. Yang, *Angew. Chem., Int. Ed. Engl.* **2012**, 51, 1420.
- [251] K. Baek, J. H. Jeong, A. Shkumatov, R. Bashir, H. Kong, *Adv. Mater.* **2013**, 25, 5568.
- [252] Y. V. Kalinin, J. S. Randhawa, D. H. Gracias, *Angew. Chem., Int. Ed. Engl.* **2011**, 50, 2549.
- [253] C. L. Randall, Y. V. Kalinin, M. Jamal, A. Shah, D. H. Gracias, *Nanomedicine* **2011**, 7, 686.
- [254] J. Park, Y. V. Kalinin, S. Kadam, C. L. Randall, D. H. Gracias, *Artif. Organs* **2013**, 37, 1059.
- [255] A. Elsayed, M. A. Remawi, N. Qinna, A. Farouk, A. Badwan, *Eur. J. Pharm. Biopharm.* **2009**, 73, 269.
- [256] T. Sadhukha, B. Layek, S. Prabha, *Drug Delivery Transl. Res.* **2018**, 8, 375.
- [257] M. B. Yatvin, W. Kreutz, B. A. Horwitz, M. Shinitzky, *Science* **1980**, 210, 1253.
- [258] U. Chitgupi, S. Shao, K. A. Carter, W.-C. Huang, J. F. Lovell, *Nano Lett.* **2018**, 18, 1331.
- [259] Z. S. Al-Ahmady, W. T. Al-Jamal, J. V. Bossche, T. T. Bui, A. F. Drake, A. J. Mason, K. Kostarelos, *ACS Nano* **2012**, 6, 9335.

- [260] K.-J. Chen, H.-F. Liang, H.-L. Chen, Y. Wang, P.-Y. Cheng, H.-L. Liu, Y. Xia, H.-W. Sung, *ACS Nano* **2013**, 7, 438.
- [261] Z. Shen, S. Mitragotri, *Pharm. Res.* **2002**, 19, 391.
- [262] H. He, X. Cao, L. J. Lee, *J. Controlled Release* **2004**, 95, 391.
- [263] H. He, J. Guan, J. L. Lee, *J. Controlled Release* **2006**, 110, 339.
- [264] K. Malachowski, J. Breger, H. R. Kwag, M. O. Wang, J. P. Fisher, F. M. Selaru, D. H. Gracias, *Angew. Chem., Int. Ed. Engl.* **2014**, 53, 8045.
- [265] F. Ilievski, A. D. Mazzeo, R. F. Shepherd, X. Chen, G. M. Whitesides, *Angew. Chem., Int. Ed. Engl.* **2011**, 50, 1890.
- [266] A. Taylor, M. Miller, M. Fok, K. Nilsson, Z. T. H. Tse, *J. Med. Devices* **2016**, 10, 020957.
- [267] K. Kuribayashi, K. Tsuchiya, Z. You, D. Tomus, M. Umemoto, T. Ito, M. Sasaki, *Mater. Sci. Eng. A* **2006**, 419, 131.
- [268] M. Zarek, N. Mansour, S. Shapira, D. Cohn, *Macromol. Rapid Commun.* **2017**, 38, 1600628.
- [269] R. F. Ismagilov, A. Schwartz, N. Bowden, G. M. Whitesides, *Angew. Chem., Int. Ed.* **2002**, 41, 652.
- [270] W. F. Paxton, K. C. Kistler, C. C. Olmeda, A. Sen, S. K. St Angelo, Y. Cao, T. E. Mallouk, P. E. Lammert, V. H. Crespi, *J. Am. Chem. Soc.* **2004**, 126, 13424.
- [271] G. A. Ozin, I. Manners, S. Fournier-Bidoz, A. Arsenault, *Adv. Mater.* **2005**, 17, 3011.
- [272] B. Xu, B. Zhang, L. Wang, G. Huang, Y. Mei, *Adv. Funct. Mater.* **2018**, 28, 1705872.
- [273] A. A. Solovev, Y. Mei, E. B. Ureña, G. Huang, O. G. Schmidt, *Small* **2009**, 5, 1688.
- [274] A. A. Solovev, S. Sanchez, Y. Mei, O. G. Schmidt, *Phys. Chem. Chem. Phys.* **2011**, 13, 10131.
- [275] V. Magdanz, G. Stoychev, L. Ionov, S. Sanchez, O. G. Schmidt, *Angew. Chem., Int. Ed. Engl.* **2014**, 53, 2673.
- [276] A. A. Solovev, W. Xi, D. H. Gracias, S. M. Harazim, C. Deneke, S. Sanchez, O. G. Schmidt, *ACS Nano* **2012**, 6, 1751.
- [277] W. Xi, A. A. Solovev, A. N. Ananth, D. H. Gracias, S. Sanchez, O. G. Schmidt, *Nanoscale* **2013**, 5, 1294.
- [278] D. Patra, S. Sengupta, W. Duan, H. Zhang, R. Pavlick, A. Sen, *Nanoscale* **2013**, 5, 1273.
- [279] W. Gao, J. Wang, *Nanoscale* **2014**, 6, 10486.
- [280] F. Peng, Y. Tu, D. A. Wilson, *Chem. Soc. Rev.* **2017**, 46, 5289.
- [281] X.-Z. Chen, B. Jang, D. Ahmed, C. Hu, C. De Marco, M. Hoop, F. Mushtaq, B. J. Nelson, S. Pané, *Adv. Mater.* **2018**, 30, 1705061.
- [282] W. Gao, B. E.-F. de Ávila, L. Zhang, J. Wang, *Adv. Drug Delivery Rev.* **2018**, 125, 94.
- [283] F. Qiu, B. J. Nelson, *Proc. Est. Acad. Sci., Eng.* **2015**, 1, 021.
- [284] H.-W. Huang, M. S. Sakar, A. J. Petruska, S. Pané, B. J. Nelson, *Nat. Commun.* **2016**, 7, 12263.
- [285] L. Zhang, J. J. Abbott, L. Dong, B. E. Kratochvil, D. Bell, B. J. Nelson, *Appl. Phys. Lett.* **2009**, 94, 064107.
- [286] M. Medina-Sánchez, L. Schwarz, A. K. Meyer, F. Hebenstreit, O. G. Schmidt, *Nano Lett.* **2016**, 16, 555.
- [287] S. Miyashita, S. Guitron, K. Yoshida, S. Li, D. D. Damian, D. Rus, in *2016 IEEE Int. Conf. on Robotics and Automation (ICRA)*, IEEE, New York, NY, USA **2016**, pp. 909–916.
- [288] J. Kim, D.-Y. Lee, S.-R. Kim, K.-J. Cho, in *2015 IEEE Int. Conf. on Robotics and Automation (ICRA)*, IEEE, New York, NY, USA **2015**, pp. 3166–3171.
- [289] T. G. Leong, C. L. Randall, B. R. Benson, N. Bassik, G. M. Stern, D. H. Gracias, *Proc. Natl. Acad. Sci. USA* **2009**, 106, 703.
- [290] E. Gultepe, S. Yamanaka, K. E. Laflin, S. Kadam, Y. Shim, A. V. Olaru, B. Limketkai, M. A. Khashab, A. N. Kalloo, D. H. Gracias, F. M. Selaru, *Gastroenterology* **2013**, 144, 691.
- [291] E. Gultepe, J. S. Randhawa, S. Kadam, S. Yamanaka, F. M. Selaru, E. J. Shin, A. N. Kalloo, D. H. Gracias, *Adv. Mater.* **2013**, 25, 514.
- [292] N. Bassik, B. T. Abebe, K. E. Laflin, D. H. Gracias, *Polymer* **2010**, 51, 6093.
- [293] N. Bassik, A. Brafman, A. M. Zarafshar, M. Jamal, D. Luvsanjav, F. M. Selaru, D. H. Gracias, *J. Am. Chem. Soc.* **2010**, 132, 16314.
- [294] A. Cangialosi, C. Yoon, J. Liu, Q. Huang, J. Guo, T. D. Nguyen, D. H. Gracias, R. Schulman, *Science* **2017**, 357, 1126.
- [295] W. Hu, G. Z. Lum, M. Mastrangeli, M. Sitti, *Nature* **2018**, 554, 81.
- [296] A. Ghosh, C. Yoon, F. Ongaro, S. Scheggi, F. M. Selaru, S. Misra, D. H. Gracias, *Front. Mech. Eng.* **2017**, 3, 7.
- [297] J. Shintake, V. Cacucciolo, D. Floreano, H. Shea, *Adv. Mater.* **2018**, 30, 1707035.
- [298] P. Anacleto, E. Gultepe, S. Gomes, P. M. Mendes, D. H. Gracias, *Technology* **2016**, 04, 120.
- [299] S. I. H. Shah, D. Lee, M. M. Tentzeris, S. Lim, *IEEE Antennas Wirel. Propag. Lett.* **2017**, 16, 848.
- [300] E. Benson, A. Mohammed, J. Gardell, S. Masich, E. Czeizler, P. Orponen, B. Högberg, *Nature* **2015**, 523, 441.
- [301] C. Myhrvold, M. Baym, N. Hanikel, L. L. Ong, J. S. Gootenberg, P. Yin, *Nat. Commun.* **2017**, 8, 14698.
- [302] D. Han, S. Pal, J. Nangreave, Z. Deng, Y. Liu, H. Yan, *Science* **2011**, 332, 342.